

WiLLM: An Open Wireless LLM Communication System

Boyi Liu
HKUST & UCL
bliubd@connect.ust.hk

Qiang Yang
University of Cambridge
qy258@cam.ac.uk

Jagmohan Chauhan
University College London
Ejagmohan.chauhan@ucl.ac.uk

Yongguang Lu
SYSU & PCL
luyg5@mail2.sysu.edu.cn

Wen Wu
Pengcheng Laboratory
wuw02@pcl.ac.cn

Jun Zhang
HKUST
ejzhang@ust.hk

Jianguo Zhao
BUPT & PCL
zhaojianguo@bupt.edu.cn

Lin Chen
Macao Polytechnic University
lchen@mpu.edu.mo

Abstract

The rapid evolution of Large Language Models (LLMs) threatens to overwhelm the existing wireless infrastructure, which calls for architectural innovations and frameworks to support the surging mobile LLM services. This paper proposes WiLLM, the first open-source wireless communication system specifically designed for LLM services, consisting of three progressive innovations. Firstly, we establish a novel paradigm by deploying LLMs in core networks (CNs) with abundant GPUs to enable distributed LLM inference services, strategically positioning LLM inference at the convergence point of the backbone bandwidth and the edges of the cellular network. Secondly, we propose an innovative extension to the conventional network slicing architecture, redefining its design with a “Tree-Branch-Fruit” framework. Its specialized adaptation for LLM services enables telecom operators to monetize these services through slice subscriptions while retaining infrastructure ownership. Finally, to operationalize this architectural vision, we present WiLLM, which systematically addresses critical limitations in existing solutions through novel key capabilities previously unattainable: (1) enhanced slice orchestration, extending existing primary slicing to implement a dual-layer slicing architecture and achieving coordinated multi-UE-multi-slice scheduling mechanisms that provide finer-grained resource allocation for LLM services; (2) universal UE compatibility through application-layer tunneling mechanisms, enabling legacy devices without native slicing capabilities to utilize LLM slice services without hardware upgrades; (3) dual-mode scheduling and cross-layer APIs, supporting flexible deployment from CNs to servers. Built on OpenAirInterface, WiLLM extends this established framework with innovations specific to LLM services, lowering the barrier for adoption by researchers without wireless expertise. Furthermore, we release the first LLM wireless communication dataset with 1,649,996 records and synchronized 58-dimensional metrics, along with two relevant benchmarks. A small but quintessential case study of smart glasses demonstrates practical viability in resource-constrained devices and human-machine interaction scenarios. WiLLM aims to build an open platform and ecosystem for cross-layer optimization and AI-telecom convergence. The code, datasets, hardwares and videos are available at <https://openwillm.github.io>.

Keywords

Large Language Model, Wireless Communication System

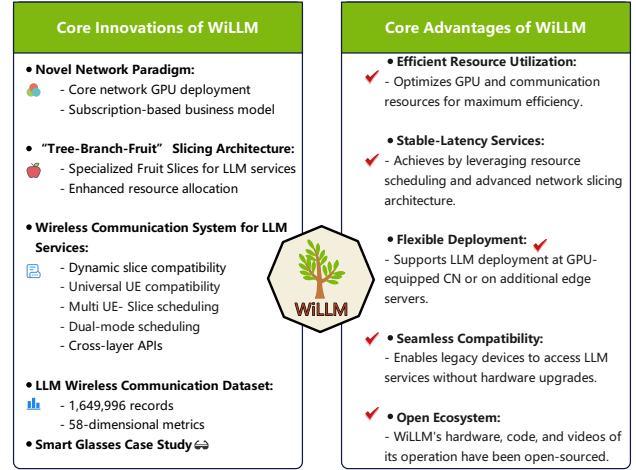


Figure 1. Contributions and advantages of the proposed WiLLM.

1 Introduction

The convergence of artificial intelligence and wireless communications represents one of the most significant technological intersections of the current decade. As computational capabilities and algorithmic sophistication continue to advance, LLMs have emerged as transformative tools with far-reaching implications across diverse application domains. The integration of these models into wireless communication systems has catalyzed a paradigm shift, enabling advanced intelligent services ranging from real-time multilingual translation to context-aware augmented reality applications [3]. As this integration accelerates, telecommunication infrastructure faces unprecedented challenges in supporting the computational demands of these resource-intensive models. Current deployments predominantly rely on either edge computing paradigms or centralized cloud processing approaches, each presenting significant limitations. Edge deployment minimizes transmission latency but suffers from constrained computational capacity and thermal limitations in user equipment (UE), while cloud-based solutions introduce unpredictable internet latency that severely impacts quality-of-experience (QoE) for interactive LLM services [36]. Moreover, the exponential growth in concurrent LLM service requests threatens to overwhelm both communication channels and computational resources, creating critical bottlenecks in service provisioning.

Recent implementations across several institutions in China, including deployments of Deepseek at multiple universities [12], demonstrate the feasibility of local LLM deployments at the network edge [4]. While these edge deployments represent a promising step toward LLM integration within

telecommunications infrastructure, they still encounter resource limitations and scalability constraints inherent to edge computing. These implementations nonetheless validate the technical viability of localized LLM services and establish a foundation for our proposed migration of LLM computational resources to the core network, where greater processing capacity and more efficient resource allocation can be leveraged. This transition from edge to core network deployment represents a natural evolution in the LLM service architecture, addressing the scalability limitations of edge deployments while maintaining the latency advantages over cloud-based solutions [6].

The current network architecture exhibits three fundamental drawbacks hindering effective LLM service integration: (1) the absence of dedicated open testbeds for LLM-specific communication scenarios, (2) the inherent conflict between centralized computation paradigms and distributed network architectures, and (3) the lack of viable business models for telecom operators in LLM service provisioning. Existing network slicing architectures provide potential foundations for addressing these challenges through resource isolation and service customization. However, conventional slicing methodologies primarily focus on traditional communication services and lack the specialized mechanisms required for computationally intensive LLM workloads [10]. Furthermore, the absence of standardized APIs and resource management frameworks inhibits the development of cross-layer optimization strategies essential for efficient LLM service delivery.

Another critical limitation is the high usability barrier of current systems. Existing platforms require specialized wireless expertise and native slicing support on user equipment, restricting access primarily to communication specialists [36]. This complexity explains why testbeds are often used only by their developer communities, significantly limiting cross-disciplinary research and broader adoption for LLM service experimentation. Moreover, the field lacks comprehensive empirical datasets capturing cross-layer performance metrics, standardized benchmarking methodologies for systematic comparison, and representative case studies demonstrating viability in resource-constrained environments. This empirical deficit perpetuates the disconnect between algorithmic innovation and operational deployment, hampering the development of generalizable principles for wireless LLM communication systems.

Motivated by the above system and networking challenges, we present WiLLM, the world’s first open-source wireless communication system specifically designed for mobile LLM services. Building upon the solid foundation provided by OpenAirInterface’s modular architecture, WiLLM strategically extends and enhances this established framework with specialized components for LLM service integration, creating a system that maintains compatibility with existing infrastructure while introducing transformative capabilities for AI-driven communications research.

The work unifies the following progressive contributions:

1.1 Paradigm

Novel Network Paradigm for LLM Services (Section 3). WiLLM establishes a novel paradigm by deploying LLMs in core networks (CNs) with GPU infrastructure, enabling distributed LLM inference services strategically positioned at the convergence point between high-bandwidth backbone connections and cellular network edges. This architectural configuration optimizes computational-communication tradeoffs while facilitating operator monetization through subscription-based network slice allocation.

1.2 Architecture

“Tree-Branch-Fruit” Slicing Architecture (Section 3.3). We propose a multi-layered slicing architecture wherein the “tree” represents foundational network infrastructure, the “branches” correspond to conventional communication service slices, and the “fruits” denote specialized LLM service slices. This architecture establishes a “slice-as-LLM-service” paradigm while maintaining compatibility with existing slicing mechanisms, achieving coordinated scheduling across multiple users and slices through cross-layer resource optimization.

1.3 System

The Wireless Communication System Specialized for LLM Service (Section 4). Based on OpenAirInterface, WiLLM implements five pivotal innovations: dynamic slice compatibility, universal UE compatibility, dual-mode resource scheduling, cross-layer API framework, and flexible deployment support. This integrated solution addresses critical limitations in existing wireless infrastructure while preserving backward compatibility.

1.4 Dataset

The World’s First LLM Wireless Communication Dataset and Benchmarks (Section 5). We introduce the first comprehensive LLM communication dataset with 1,649,996 records, each containing 58 communication metrics synchronized across UE-gNB-CN interfaces. This enables holistic cross-layer analysis of LLM communication patterns. In addition, we present two metrics, LAREI and LSEQ, as benchmarks that offer a standardized methodology for wireless LLM service evaluation.

1.5 Case Study

Smart Glasses Case Study (Section 6). The practical utility of WiLLM is validated through a smart glasses application that implements gesture-triggered queries and scene interpretation. Based on the principle of user-perceived continuity in human-computer interaction, we establish a response latency target of approximately 2 seconds, achieving optimal slicing through offline statistical analysis and online learning methodologies.

2 Related Work and Comparison

2.1 Wireless Communication for LLM

The convergence of LLMs with wireless systems has precipitated prolific theoretical advancements characterized by a critical implementation deficit. Despite many approaches being proposed, the field confronts a fundamental disjunction between algorithmic innovation and operational realization.

Architectural paradigms manifest in three configurations: 1. Cloud-edge frameworks [8] [31] [11] establish a hierarchical computational distribution by allocating processing tasks between the cloud and edge devices. This approach combines the high computational power of the cloud with the low latency characteristics of the edge. For example, NetGPT [8] relies on cloud-edge collaboration in personalized generative services. However, the dynamic nature of wireless channels limits its adaptability. Reference [31] explores the potential of cloud-edge computing, while [11] highlights the challenges of implementing edge AI generated from cloud-based LLMs. 2. Edge computing deployment [5] [22] [30] runs LLMs directly on edge servers or devices, enhancing performance through quantization techniques. For instance, Edge-LLM [5] optimizes edge adaptability using unified compression and adaptive layer voting, while [22] demonstrates hardware-supported edge deployment cases. Nevertheless, the limited capacity of edge devices remains a bottleneck, as further validated in [30]. 3. Distributed architectures [33] [20] decompose LLM computational tasks across multiple nodes to fully utilize distributed resources. For example, WDMoE [33] proposes a wireless distributed framework based on mixture-of-experts, though its validation in congested scenarios remains insufficient.

Resource optimization methodologies span cross-modal approaches (JPPO [34]) integrating prompt compression with power optimization; adaptive partitioning strategies [7] reconfiguring computational boundaries under network fluctuations; and collaborative frameworks [16] optimizing offloading decisions across distributed resources. Service integration architectures encompass specialized slicing methodologies (LLM-Slice [19]), intelligent orchestration approaches [9], and long-context integration strategies [32, 35].

Bottlenecks and our solutions: The field faces three bottlenecks: theory-centric validation lacking real-world relevance, insufficient cross-layer integration, and unproven business viability. WiLLM addresses these through an empirical platform bridging theory and implementation. Unlike conventional edge server strategies that incur coordination inefficiencies, we deploy LLMs on GPU-equipped infrastructure at the backhaul-RAN nexus, enhancing computational capacity, resource optimization, and infrastructure integration.

2.2 Related Systems and Comparisons

In this section, we evaluate prominent open-source systems for their capabilities across a range of technical features essential for modern wireless networks, including OAI,

srsRAN, Open5GS, FlexRIC, and Janus. While these systems contribute significantly to wireless network research and development, they exhibit limitations in fully supporting the comprehensive demands of next-generation networks. OAI provides a complete 4G/5G protocol stack implementation, spanning from the physical layer to the network layer. Its modular design supports academic research and prototyping [23]. srsRAN is a lightweight and highly customizable 4G/5G software suite [15], offering flexibility in scheduling and QoS management. Open5GS implements comprehensive 5G core network functions, including AMF, SMF, and UPF components [2], establishing a solid foundation for network integration. FlexRIC is a programmable RAN SDK focused on 5G multi-tenancy and low-latency optimization [29]. Janus is a programmable RAN platform developed by Microsoft, based on the O-RAN architecture, supporting dynamic service models [14]. While these systems offer essential assistance in certain aspects of wireless networking, they exhibit inadequate support for general technical features like UE compatibility, slice flexibility, and specialized support for LLM communications, etc. Detailed objective metric comparisons are presented in Table 2 and Table 1 in the Appendix.

2.2.1 Research Gaps and Positioning of WiLLM

While existing open-source communication platforms provide valuable research infrastructure, comprehensive analysis reveals significant operability impediments that restrict their adoption beyond specialized research communities. As quantified in Table 1 and 2, current systems demonstrate substantial limitations in critical usability dimensions. The requirement for native slicing support at the UE level presents a particularly problematic constraint, effectively excluding standard commercial devices without specialized protocol modifications [1, 28]. This limitation fundamentally contradicts the purpose of experimental testbeds, which should facilitate algorithm validation across diverse implementation scenarios rather than constraining experimental configurations to narrow protocol-specific deployments. Furthermore, these resulted in an undesirable ecosystem fragmentation where testbeds remain utilized primarily by their own development communities, significantly limiting cross-disciplinary innovation.

WiLLM aims to bridge the technological gap between wireless communication and LLM systems by extending the OAI architecture to build the first open-source wireless communication system designed specifically for LLM services.

3 Paradigm

LLMs as transformative technologies in wireless communications call for fundamental network architecture reconceptualization. Despite edge computing's partial success in LLM deployment, its device-centric approach inherently limits scalability and optimization. We propose a novel core network paradigm that positions LLM resources at the nexus of high-capacity backhaul and wireless access networks,

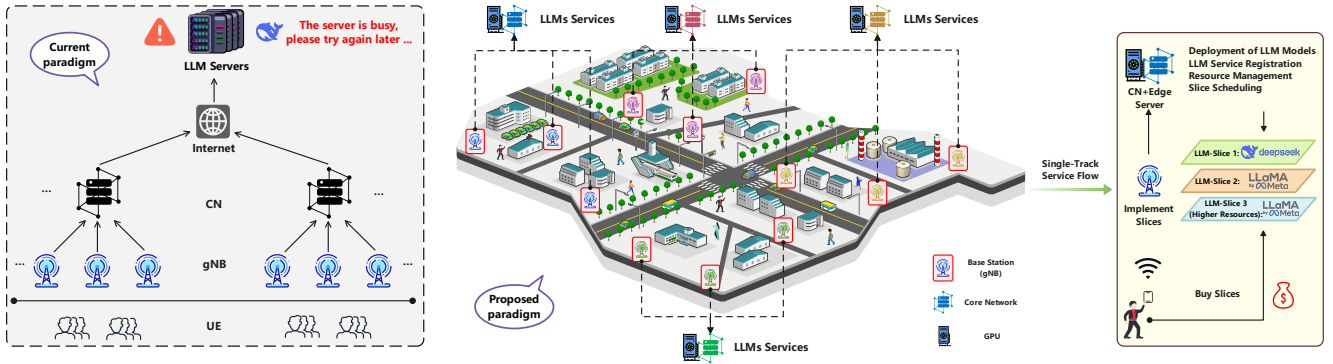


Figure 2. Left: Conventional cloud-based LLM service deployment architecture with internet connectivity. Right: Proposed core network LLM service deployment architecture with GPU resources at network convergence points.

enabling comprehensive computational-communication resource integration that transcends traditional edge computing constraints.

3.1 Deployment Paradigm for LLM Services

Current LLM service deployment architectures exhibit fundamental architectural limitations that constrain their performance envelopes. As illustrated in Figure 2, traditional cloud-based configurations necessitate traversal of multiple network boundaries: from UE through gNB and CN to remote LLM servers via public internet infrastructure. This architectural paradigm introduces non-deterministic network latency due to Internet Gateway traversal, unpredictable congestion during peak utilization periods, and critically, a decoupling of computational and communication resource management planes that prevents cross-layer optimization.

Our proposed paradigm, depicted in the right section of Figure 2, implements a strategic reconfiguration wherein GPU resources are directly integrated within the core network infrastructure. This implementation positions LLM computational capabilities precisely at the convergence point between high-bandwidth backbone connections and cellular network edges. Technically, this architecture establishes a single-track service flow where UE requests traverse a deterministic path (UE→gNB→CN with integrated GPU) rather than extending through variable internet routes. The implementation incorporates dedicated GPU modules within the core network nodes, connected via high-speed backplane interconnects to the CN’s packet processing infrastructure. This architectural positioning enables packet processing, slice scheduling, and LLM inference to occur within the same administrative domain, eliminating inter-domain traversal overhead that characterizes cloud deployments while providing computational density unattainable in resource-constrained edge implementations.

The technical implementation comprises three principal architectural components:

- (1) **Deterministic Service Path Integration:** As shown in Figure 2, our implementation establishes a direct service flow from UE through gNB to the CN-GPU integrated

infrastructure. This configuration eliminates the indeterministic routing and potential congestion points inherent in public internet traversal, enabling guaranteed service-level agreement enforcement through contiguous administrative control of the entire transmission path.

- (2) **Hierarchical Slice-Based Resource Orchestration:** The implementation leverages the slice management mechanisms detailed in Section 3.3 to establish fine-grained coordination between communication and computational resources. Rather than treating these as separate resource domains (as in conventional implementations), our architecture implements a unified resource allocation framework where slice policies govern both radio resource allocation at the gNB and computational resource distribution at the CN-GPU nexus.
- (3) **End-to-End Service Flow Management:** The architecture implements a comprehensive flow control mechanism that extends from UE request initiation through transmission scheduling, computational resource allocation, and response delivery. This coordinated approach enables advanced optimization techniques such as predictive resource allocation, where the system anticipates computational requirements based on request characteristics and proactively configures both network and computational resources accordingly.

3.2 Transcending Edge Computing Limitations

The core network deployment paradigm for LLM services introduces fundamental architectural, operational, and infrastructural enhancements that transcend edge computing’s intrinsic limitations. The hierarchical “Tree-Branch-Fruit” slicing framework (Section 3.3) enables differentiated, SLA-governed LLM orchestration, surpassing edge computing’s localized resource allocation. The cross-layer optimization framework (Sections 4.2) synergistically coordinates resources across network strata, realizing dynamic adaptation unattainable through edge computing’s device-centricity. Strategic LLM resource placement at the backhaul-RAN confluence forges a computational-communication symbiosis, transcending edge deployments’ latency-processing trade-offs. Empirical insights from the WiLLM dataset (Sections 5)

corroborate the core network paradigm’s transformative potential, illuminating performance benefits and optimization opportunities eclipsing edge computing. This paradigm establishes the foundation for the “Tree-Branch-Fruit” slicing architecture, facilitating a technical environment where both communication resources and computational capabilities can be allocated through unified slice policies. The implementation enables an evolutionary deployment path that preserves investment in existing infrastructure while advancing sophisticated LLM service delivery models.

3.3 “Tree-Branch-Fruit” Slicing Architecture

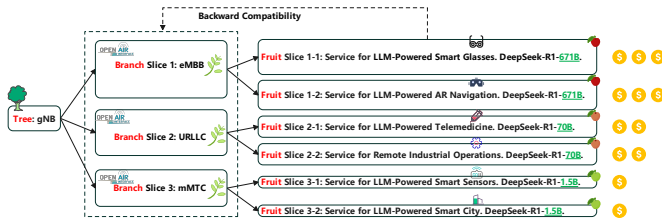


Figure 3. Tree-Branch-Fruit network slicing architecture with hierarchical service organization.

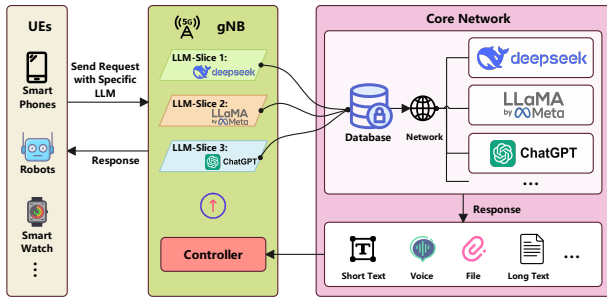


Figure 4. Slice function architecture of WiLLM with integrated UE, gNB, Core Network, and Edge Server Components [19].

Building upon our core network deployment paradigm, we propose a novel “Tree-Branch-Fruit” slicing architecture that transforms conventional network slicing approaches into a comprehensive service provisioning platform. This multi-tier architecture, illustrated in Figure. 3, establishes a hierarchical framework that maintains backward compatibility with existing slicing mechanisms while introducing specialized LLM service slices. In this architecture:

- **Tree (gNB):** Represents the foundational radio access network infrastructure, serving as the common entry point for all network traffic and the root of the slicing hierarchy.
- **Branch Slices:** Correspond to traditional communication service slices defined in 5G standards, including enhanced Mobile Broadband (eMBB), Ultra-Reliable Low-Latency Communication (URLLC), and massive Machine Type Communication (mMTC). These branch slices are not the focus and implementations of this work. These branches maintain backward compatibility with existing network functions.

- **Fruit Slices:** Denote specialized LLM service slices that extend from branch slices, each configured for specific application domains and computational requirements. Figure. 3 presents illustrative examples of potential fruit slice configurations, including various LLM service use cases with different model sizes tailored to specific application requirements.

The examples illustrated in Figure. 4 demonstrate how different application domains might be served by appropriately sized language models, with computationally intensive applications connected to branches supporting higher bandwidth and more powerful models, while lightweight IoT applications utilize smaller, more efficient models. These examples are not prescriptive implementations but rather illustrative use cases demonstrating the flexibility of the proposed architecture. This architecture establishes a “slice-as-a-LLM-service” paradigm that facilitates efficient multi-user and multi-slice coordinated scheduling through cross-layer resource optimization. The hierarchical structure enables:

- **Differentiated Service Provisioning:** Telecom operators can provide LLM services with varying performance guarantees and computational capacities tailored to specific application requirements and price points.
- **Resource Isolation:** The architecture enforces strict isolation between service slices, preventing performance degradation in one service from affecting others and enabling guaranteed quality-of-service levels.
- **Domain-Specific Optimization:** Each fruit slice can be independently optimized for its specific application domain, with tailored model selection, inference parameters, and resource allocation strategies.
- **Modular Service Evolution:** New LLM services can be deployed as additional fruit slices without disrupting existing services, facilitating incremental innovation. Our architecture achieves forward compatibility via application-layer tunneling that transcends conventional slicing constraints. This method encapsulates LLM traffic within standard application protocols, enabling infrastructure compatibility while maintaining architectural autonomy. The approach provides telecommunications operators with implementation flexibility independent of underlying radio network slice capabilities. This strategic decoupling of service implementation from network infrastructure allows fruit slices to evolve asynchronously from hardware upgrade cycles or standardization timelines. Such architectural independence ensures operational resilience across heterogeneous networks, enabling deployment of novel LLM capabilities unfettered by the limitations of conventional slicing frameworks.

The monetary value icons associated with different fruit slices in Figure. 3 illustrate the differentiated pricing potential of this architecture, with higher-resource slices commanding premium pricing while lightweight services remain cost-effective for mass deployment. This economic framework

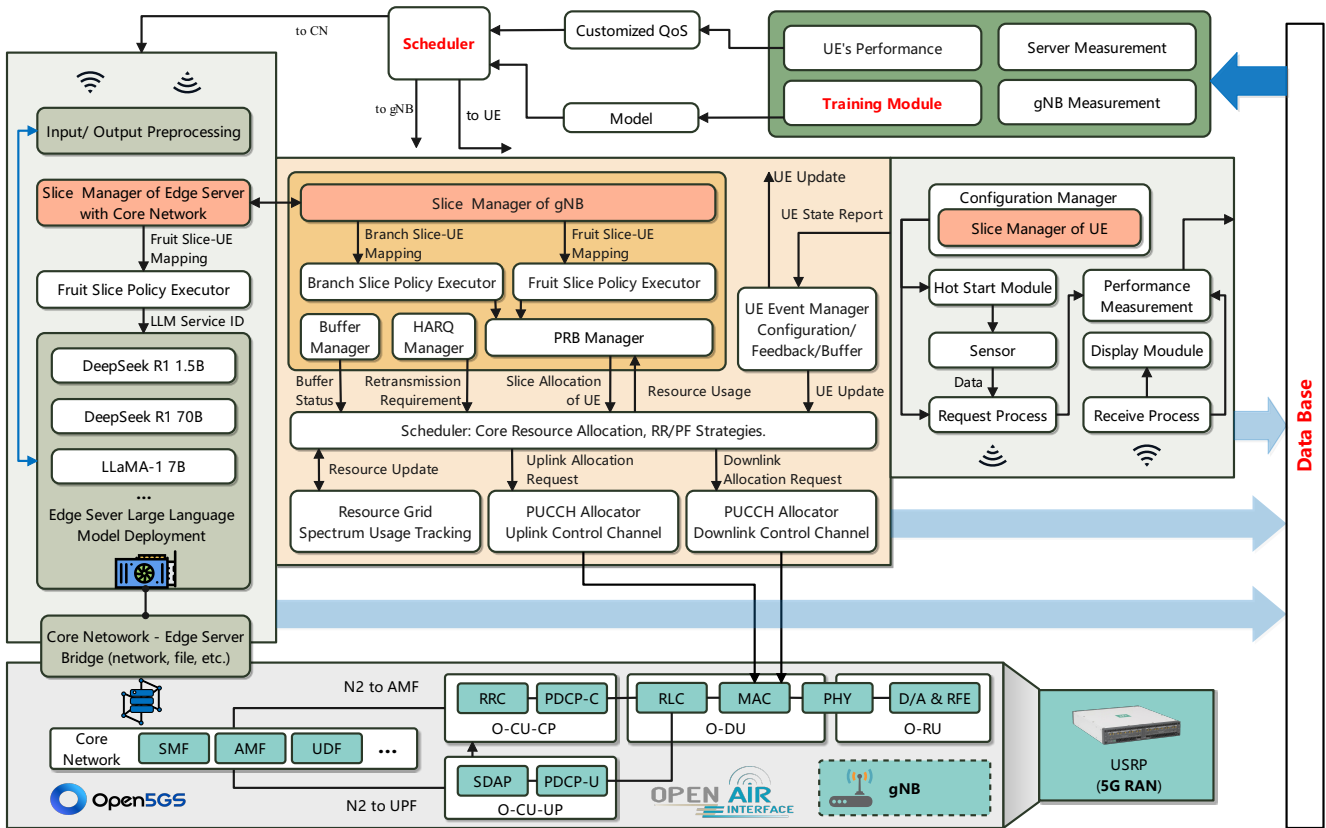


Figure 5. Comprehensive system architecture of WiLLM with UE, gNB, CN, and Edge Server Components.

creates sustainable incentives for network operators to invest in LLM-capable infrastructure.

The “Tree-Branch-Fruit” architecture represents an advancement over conventional slicing approaches by introducing application-specific service customization while maintaining backward compatibility with existing network functions. This novel paradigm establishes the foundation for our comprehensive WiLLM implementation, which will be detailed in subsequent sections.

4 The Proposed System

This section presents the comprehensive design and implementation of WiLLM, our novel wireless communication system specifically optimized for LLM service delivery. Building upon the “Tree-Branch-Fruit” slicing architecture described in Section 3, we have constructed a complete system implementation that extends the OpenAirInterface framework with specialized components for LLM service provisioning. Figure. 5 illustrates the system architecture, encompassing UE, gNB, core network, and edge server components with their associated interconnections and functional modules.

4.1 System Architecture Overview

WiLLM adopts an innovative vertical integration architecture design, achieving end-to-end coordination from user applications to core networks through a hierarchical management framework. This architecture, centered on layered slice management, organically integrates four key subsystems:

the **CN subsystem** built on the Open5GS framework, with enhanced edge computing capabilities through a dedicated Edge Server Bridge; the **gNB subsystem** that implements enhanced “Tree-Branch-Fruit” slice management mechanisms based on OpenAirInterface; the **UE subsystem** that integrates configuration management, slice control, and performance measurement function modules; and the **edge server subsystem** that carries various LLM deployments and executes corresponding slice policies. These subsystems are not simply stacked together but are tightly coupled through a hierarchical slice management framework, enabling precise scheduling and collaborative optimization of cross-layer resources, thereby ensuring the efficiency of the LLM communication system.

4.2 Implementation Framework

WiLLM extends OpenAirInterface with strategic innovations that balance implementation efficiency with transformative functionality. This approach leverages established communication foundations while introducing specialized components that fundamentally transform system capabilities:

4.2.1 Dynamic Slice Compatibility

As illustrated in Figure. 5, our implementation extends conventional network slicing capabilities with LLM-specific service slices while maintaining backward compatibility. The Slice Manager of gNB encompasses both Branch Slice-UE

Mapping and Fruit Slice-UE Mapping components, with bidirectional data flows (indicated by the UE Update and UE State Report pathways) enabling dynamic reassignment of resources in response to changing service demands.

The implementation employs a virtualization layer that abstracts underlying slice implementation details, while the Branch Slice Policy Executor and Fruit Slice Policy Executor enforce service-specific policies at the gNB level. As shown in the left section of Figure. 5, these policy executors interact directly with the PRB Manager, creating a decision hierarchy that translates high-level service policies into physical resource allocations.

4.2.2 Universal UE Compatibility

To address the limitations of current UE implementations, which often lack native slicing capabilities, WiLLM incorporates a middleware-based slice access mechanism through the Slice Manager of UE component. The data flow illustrated in Figure. 5 demonstrates how this component interfaces with both the Configuration Manager and Hot Start Module, enabling UEs without native slicing support to access specialized LLM services through application-layer tunneling techniques that encapsulate service traffic within standard data streams.

This compatibility layer effectively bypasses the limitations of current community implementations of primary slicing, which remain incomplete and inconsistently supported across device ecosystems, thereby expanding the addressable user base for LLM services.

4.2.3 Multi-UE Multi-Slice Scheduling Capability

WiLLM implements a comprehensive multi-UE-multi-slice coordinated scheduling mechanism that operates through a two-phase process. The Scheduler module in Figure. 5 forms the nexus of this coordination, receiving inputs from multiple sources including the Buffer Manager (which provides Buffer Status information), HARQ Manager (which signals Retransmission Requirements), and the Slice Allocation of UE component.

The multi-UE-multi-slice coordination operates through a two-phase process:

- A global allocation phase distributes available physical resource blocks across active slices according to their relative priorities and resource guarantees.
- An intra-slice scheduling phase allocates resources to individual UEs within each slice based on service-specific metrics.

This hierarchical approach ensures fair and efficient resource utilization while maintaining service isolation, effectively enabling legacy devices to benefit from slice-specific performance guarantees without hardware modifications.

4.2.4 Dual-Mode Resource Scheduling

WiLLM implements complementary “*separated*” and “*embedded*” resource scheduling methodologies to accommodate diverse operational requirements and infrastructure constraints:

- **Embedded Scheduling Mode:** The embedded approach implements slice-aware resource allocation directly within the scheduler pipeline, as formalized in Algorithm 1. Figure. 5 illustrates how this approach integrates with the Resource Grid and Spectrum Usage Tracking components to maintain awareness of physical layer constraints while implementing policy decisions.
- **Separated Scheduling Mode:** The separated approach decouples slice-specific policy decisions from core scheduling logic, employing an external decision engine that solves a global optimization problem and subject to resource constraints and slice isolation requirements. The data flow in Figure. 5 shows how the Resource Update pathway enables this external engine to maintain synchronization with the core scheduling system.

The interaction between the Uplink/Downlink Allocation Request pathways and the PUCCH Allocator modules for both uplink and downlink control channels (as depicted in Figure. 5) demonstrates how the system coordinates the allocation of scarce control channel resources across multiple UEs and slices.

4.2.5 Cross-Layer API Framework

WiLLM introduces a comprehensive API architecture (detailed in Figure. 16) that facilitates vertical integration between application requirements and network-level resource allocation. As shown in Figure. 5, this framework enables multiple feedback pathways:

- (1) **Performance Feedback Loop:** The UE State Report, Configuration/Feedback/Buffer, and UE Update connections establish a closed-loop feedback system that continuously monitors service performance and adapts resource allocation accordingly. The bidirectional nature of these connections, clearly depicted in Figure. 5, enables adaptive behavior at multiple timescales.
- (2) **Service-Specific Optimization:** The LLM Service ID mechanism enables adaptation of network parameters based on computational characteristics of different LLM implementations. Figure. 5 illustrates how this information flows from the Edge Server Subsystem through the Slice Manager to influence allocation decisions.
- (3) **Resource Utilization Monitoring:** The Resource Usage and Slice Allocation connections provide visibility into consumption patterns, establishing a cross-layer information flow that informs both immediate scheduling decisions and longer-term policy refinements.

4.2.6 Deployment Flexibility

The system supports flexible LLM deployment configurations, with the Edge Server Large Language Model Deployment component hosting multiple LLM variants with different parameter sizes as shown in Figure. 5, and the CN-Edge Server Bridge facilitating seamless integration between computational resources and network infrastructure through standardized file and network interfaces.

4.3 The Database Module

A distinctive feature of WiLLM is its integrated data collection module (shown in the upper section of Figure. 5), which continuously refines resource allocation strategies based on operational metrics. This module creates a meta-feedback loop that transcends individual communication sessions, collecting performance data from UE’s Performance, gNB Measurement, and Server Measurement components to inform the evolution of the Customized QoS Scheduler and Model components.

The system incorporates a comprehensive Database component (illustrated in the right section of Figure. 5) that persistently stores operational metrics, enabling longitudinal analysis of system performance. This data repository serves as both an analytical resource for offline optimization and a training corpus for online learning algorithms.

4.4 System Validation Infrastructure

To validate practical performance, we deployed a fully functional testbed (Figure.14 in Appendix) integrating a complete wireless communication chain with LLM service deployment. Following the logical architecture shown in Figure. 5, the core computing infrastructure employs an Intel Core i9-14900KF processor as gNB host, USRP B210 for RF frontend, and NVIDIA RTX 4090 GPU for LLM inference, supporting multi-user, multi-slice concurrent testing scenarios. The system’s operational status can be monitored through a custom GUI (Figure. 15 in Appendix). This configuration achieves complete system integration from radio access to core network, providing an ideal environment for evaluating WiLLM in practical deployments.

5 The WiLLM Dataset

We present the first comprehensive LLM communication dataset with synchronized metrics, enabling reproducible research and systematic evaluation. Appendix F details components, acquisition, synchronization, and error descriptions.

5.1 Dataset Metrics Overview

Our dataset contains 1,649,996 records with 58 metrics spanning the LLM service delivery chain. It covers four scenarios: static UE and gNB (290,653 records), dynamic UE and static gNB (363,906 records), static UE and dynamic gNB (430,369 records), and dynamic UE and gNB (565,068 records). “Dynamic” indicates dynamically allocated network slices, while “static” indicates invariant parameters throughout measurements. The dataset includes 22 metrics at the user equipment layer, 25 at the wireless access network layer, and 18 at the edge server layer.

Figures 17 and 18 confirm stable base station power and noise levels during data collection. We implemented NTP-based distributed synchronization, calibrating all devices through a common server for microsecond-level sampling precision. By recording timestamps at both the UE and server endpoints and using latency compensation algorithms, we maintained synchronization errors within ± 1.0 milliseconds.

5.2 Metric Architecture

The dataset provides synchronized metrics across three architectural layers: **UE Metrics (Appendix Table 4)** capture end-user experience through latency, timing, resolution, modalities, and payload characteristics; **gNB Metrics (Appendix Table 6)** document wireless conditions via radio parameters (MCS, CQI, BLER), resource allocation, transmission performance, and slice configuration; and **CN with Edge Server Metrics (Appendix Table 5)** measure computational aspects through inference timing, token processing, model loading, and response generation. The dataset’s value lies in its temporal synchronization, enabling precise correlation between user experience, network conditions, and computational performance. This facilitates advanced research: developing ML models for scheduling, implementing data-driven allocation, creating cross-layer analytics, and validating theoretical models. This corpus establishes a foundation for reproducible research in wireless systems supporting LLM services.

5.3 Preliminary Findings and Conclusions

This section presents preliminary findings derived from our dataset, with particular focus on communication directionality characteristics and the impact of network slicing on performance metrics.

5.3.1 Uplink vs. Downlink Characteristic Analysis

Finding 1: Our dataset reveals distinct performance profiles for uplink and downlink communication scenarios. In the uplink case (UE image request \rightarrow LLM inference \rightarrow text response), as visualized in Figure. 6, we observe that inference time constitutes a substantial proportion of the total processing latency (74-87% across resolution groups). The relative contribution of uplink transmission time marginally increases (11-25%) with the rise in resolution.

Finding 2: In contrast, the downlink scenarios (text request \rightarrow LLM text response \rightarrow image response), depicted in Figure. 7, demonstrate markedly different characteristics. Downlink transmission time dominates the overall latency budget (81-86%), with inference time contributing a significantly smaller proportion (12-17%).

Conclusions: These directional performance characteristics validate WiLLM’s “Tree-Branch-Fruit” slicing architecture and LLM deployment paradigm in several critical ways:

- (1) In the uplink scenario, the largest delay comes from inference time, followed by uplink transmission time. This finding supports our strategy of deploying LLMs with GPUs in the CN. This is achieved by reducing the inference time through distributed LLM processing at the CN and minimizing uplink transmission delays by staying close to users, thereby avoiding the need to go through the public Internet.
- (2) The pronounced asymmetry between uplink and downlink transmission characteristics empirically validates our

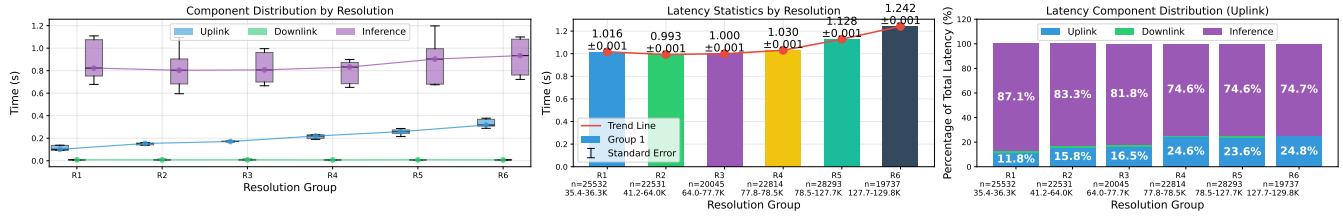


Figure 6. Component distribution and latency analysis for uplink transmissions across resolution groups. The x-axis labels R1 - R6 represent various resolution groups for image requests sent to LLM, where R1 - R6 correspond to increasing resolutions, with “n” representing the sample size per group, and the lower value of “n” indicating the resolution range for each group. The left panel shows the temporal distribution of communication components (uplink, downlink, inference), the center panel presents statistical trends with standard errors, and the right panel quantifies each component’s percentage contribution to total latency, illustrating how higher resolutions affect time allocation in the transmission pipeline.

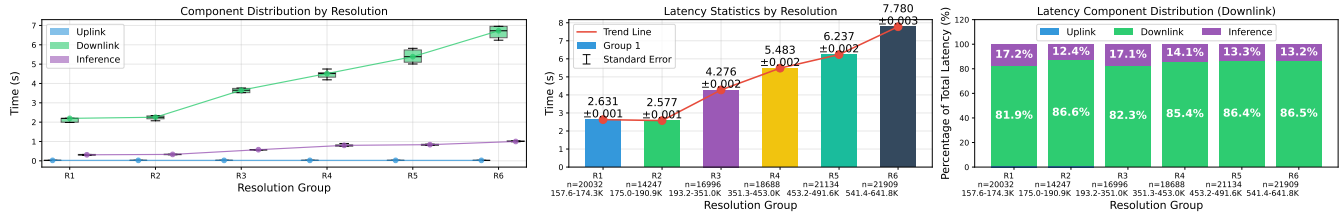


Figure 7. Component distribution and latency analysis for downlink transmissions across resolution groups. This figure illustrates the temporal characteristics of downlink transmissions stratified by resolution groupings. Similar to Figure 6, it provides three complementary views: component distribution, statistical latency metrics, and proportional component analysis. All legend elements in the figure remain consistent with Figure 6, with the only distinction being the utilization of downlink samples.

“Fruit Slice” architectural paradigm, confirming that effective monetization of LLM services requires direction-specific slice configurations that independently optimize bandwidth and computation intensive workloads, a capability that is not achievable through conventional slicing approaches.

- (3) The pronounced resource requirement asymmetry between uplink and downlink scenarios provides compelling empirical justification for direction-specific scheduling mechanisms. These findings validate the architectural necessity of dual-mode scheduling capabilities, confirming that efficient LLM service delivery requires dynamic, direction-aware resource provisioning rather than single-direction allocation policies. This increased flexibility in provisioning is a key enabler of the slice-based monetization framework.

These insights reveal that WiLLM’s paradigm and architecture, substantiated by real-world datasets, demonstrate critical advantages over conventional systems in operational dimensions. These advancements provide a robust framework for direction-specific resource optimization that traditional wireless systems cannot achieve. We provide further analysis of the reasons for the experimental phenomenon and additional notes in the appendix F.1.

5.3.2 Network Slicing Impact Analysis

Finding 3: The effectiveness of our “Tree-Branch-Fruit” slicing architecture is demonstrated through comparative analysis of network performance under different slicing configurations. Figure 8 illustrates how slice configuration affects the

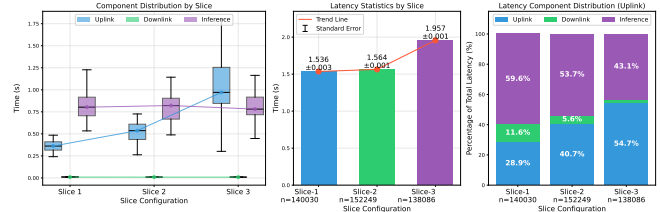


Figure 8. Component distribution and latency analysis across slice groups. In the figure, the communication resources for uplink slices in Slice 1 to Slice 3 are gradually increasing. This examines performance impacts of different slice configurations on communication component distribution, highlighting distinct latency profiles for three configurations. The middle panel statistically validates performance differences, while the rightmost panel quantifies how slice configurations shift processing time proportions among uplink, downlink, and inference operations.

temporal distribution of processing components, with notable variations in inference time allocation (43.1% to 59.6%) and uplink transmission time (28.9% to 54.7%) across different slicing arrangements. This demonstrates that slicing indeed affects the latency of LLM communication services and its components, which supports WiLLM’s paradigm.

Finding 4: Examining PRB allocation patterns in Figure 9 alongside actual byte transmission data in Figure 10 reveals critical insights into slicing efficiency. Our implementation successfully achieves differentiated PRB allocation conforming to slice policies. Moreover, there exists a discrepancy between theoretical resource allocation and actual transmission patterns. Specifically, byte traffic does not scale proportionally with PRB allocation, suggesting potential resource utilization inefficiencies within the slicing framework. This

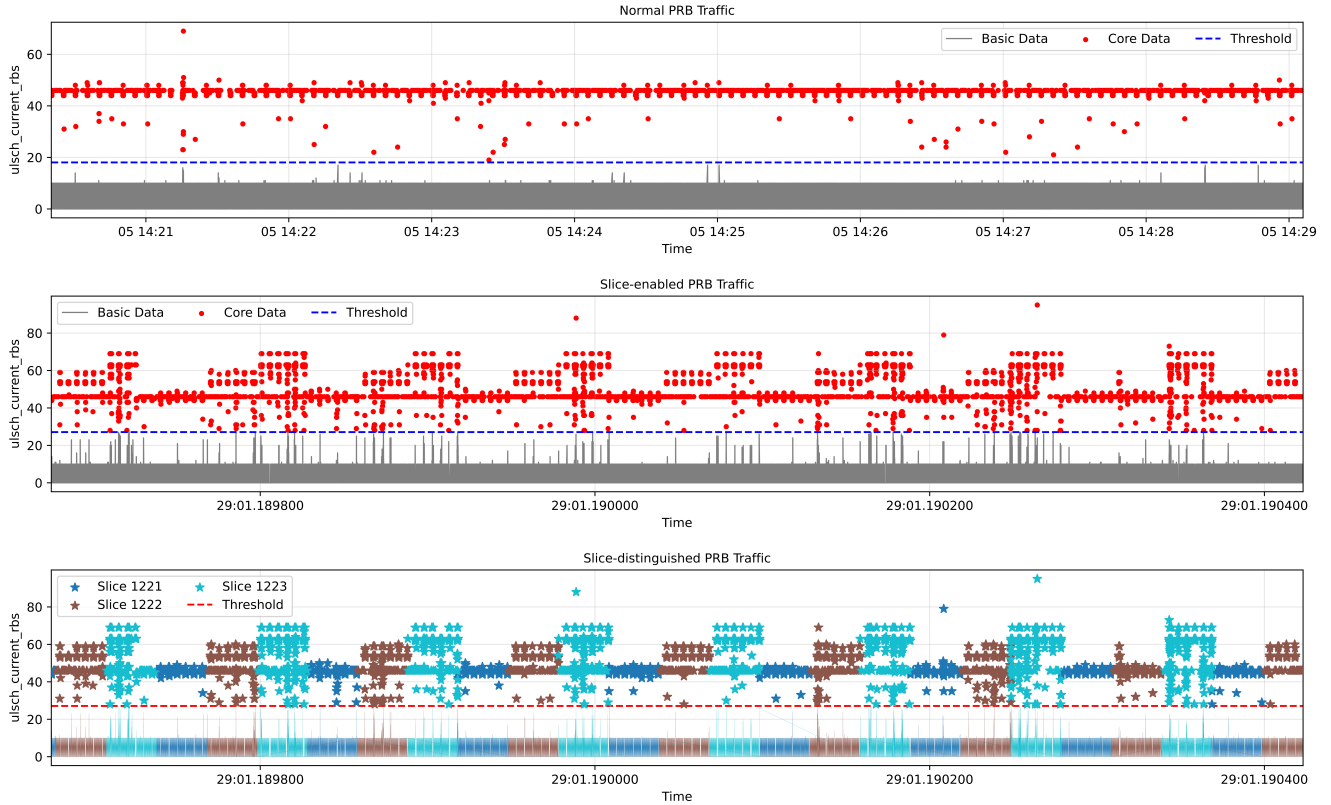


Figure 9. This figure presents a temporal analysis of PRB allocation patterns across three implementation scenarios: normal traffic (top), slice-enabled traffic (middle), and slice-distinguished traffic (bottom). The x-axis represents timestamps in microseconds, while the y-axis denotes “ulsch_current_rbs”, indicating the current number of resource blocks allocated to the UE. The visualization demonstrates the effectiveness of the slicing architecture in providing differentiated resource allocation while maintaining threshold compliance, with slice-distinguished traffic showing clear separation between service classes. The area below the dashed line is labeled as “basic data” with no data transmission, while the area above corresponds to “core data”.

indicates that due to the complex interplay of elements affecting communication, system execution mechanisms, and varying UE requests, PRB and actual communication bytes are not strictly linearly correlated.

Conclusions: These empirical observations demonstrate the critical value of WiLLM in several dimensions:

- (1) The significant variability in component allocation across slice configurations validates that WiLLM’s “Tree-Branch-Fruit” architecture enables effective LLM-specific service slicing, supporting our proposed diverse pricing patterns and underscoring the necessity of finer-grained resource allocation mechanisms.
- (2) The observed allocation-utilization gap reveals that theoretical and simulation-based approaches often fail to capture real-world complexities, confirming WiLLM’s role as an essential empirical platform bridging theory and implementation.
- (3) The non-linear relationship between resource allocation and actual transmission performance underscores the necessity of WiLLM’s cross-layer API framework and dual-mode scheduling capabilities, which enable adaptive optimization based on observed rather than simulated performance patterns.

The analysis of the causes of the observed phenomenon is presented in the Appendix F.2.

These findings substantiate WiLLM’s fundamental contribution: while traditional approaches rely on simplified resource allocation models, our system provides the empirical foundation and architectural flexibility required for truly efficient LLM service delivery in wireless environments. This empirical grounding enables telecommunications operators to achieve differentiated service quality and optimal resource utilization, a critical requirement for commercially viable LLM wireless services.

5.4 Benchmark

Analyzing datasets reveals intricate dependencies among communication resources, computational capacity, and service quality, requiring specialized metrics. As traditional network metrics fail to capture LLM service delivery’s multi-dimensional nature, we propose two complementary metrics for evaluating LLM wireless communication systems. The LLM-Aware Resource Efficiency Index (LAREI) quantifies the efficiency relationship between request complexity, computational demands, and resource utilization:

$$\text{LAREI} = \frac{\text{RDV} \cdot \log(1 + \text{LLM_Para})}{\text{Resources} \cdot \text{Latency}} \cdot \omega$$

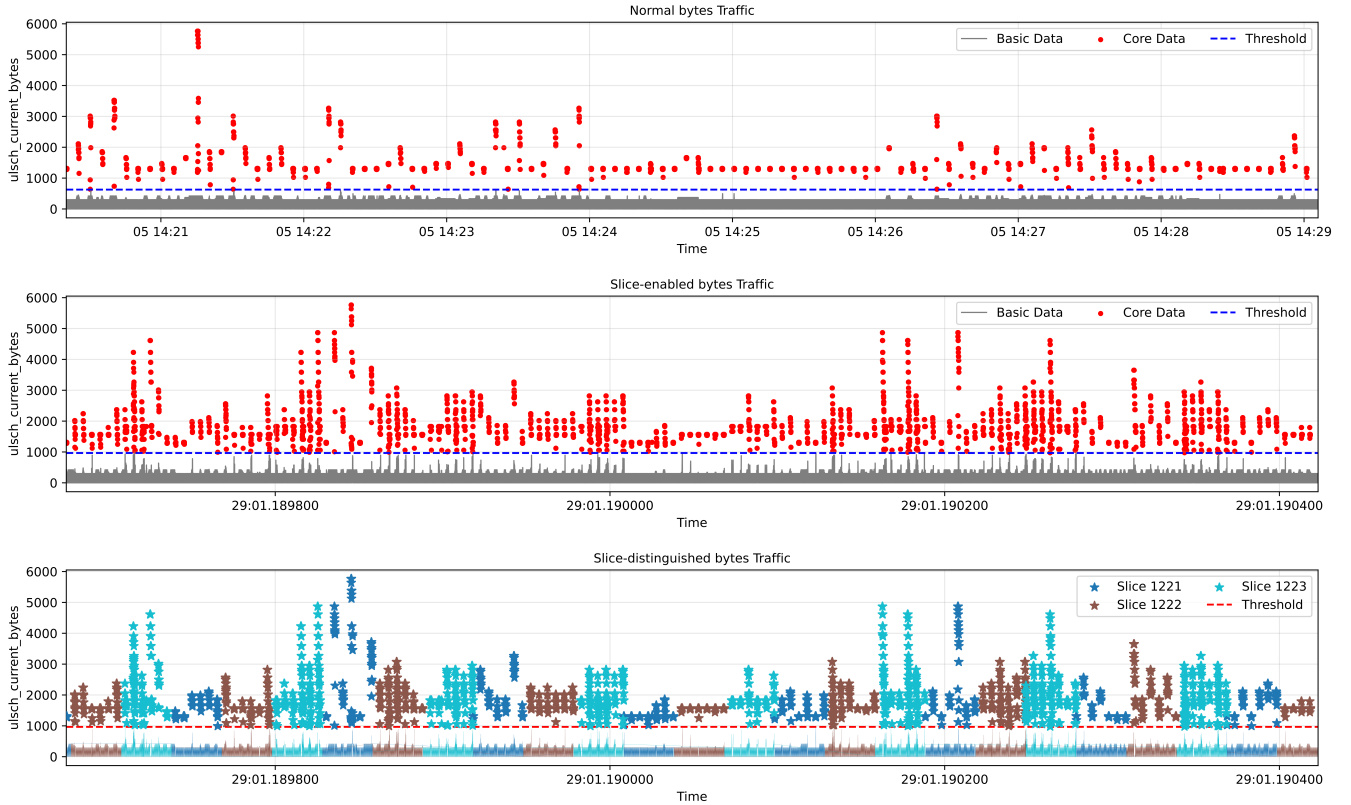


Figure 10. The figure illustrates a temporal analysis of PRB allocation patterns across three scenarios: normal traffic (top), slice-enabled traffic (middle), and slice-distinguished traffic (bottom). The x-axis represents timestamps in microseconds, while the y-axis denotes “usch_current_bytes”, indicating the current transmitted bytes of the UE.

Where RDV is request data volume, LLM_Para represents model complexity in billions of parameters, Resources denotes allocated communication resources, Latency indicates end-to-end response time, and ω is a normalization coefficient.

For slicing effectiveness evaluation, we introduce the LLM Slice Efficiency Quotient (LSEQ):

$$\text{LSEQ} = \frac{\text{RDV_slice} \cdot (1 - \text{Error Rate}) \cdot \sqrt{\text{LLM_Para_slice}}}{\text{Slice Resources}} \cdot \delta$$

This metric combines slice-specific data volume (RDV_slice), transmission reliability (1 - Error Rate), computational complexity (represented by $\sqrt{\text{LLM_Para_slice}}$, reflecting diminishing returns through square root scaling), and allocated slice resources (Slice Resources), all normalized by the parameter δ .

These metrics establish a framework for evaluating and optimizing wireless LLM communication systems, balancing computational sophistication with communication efficiency.

Detailed analysis is presented in Appendix G.

6 A Case Study of Smart Glasses

6.1 Smart Glasses Integrated in WiLLM

To validate WiLLM’s effectiveness in real-world applications, we implemented a small but quintessential case

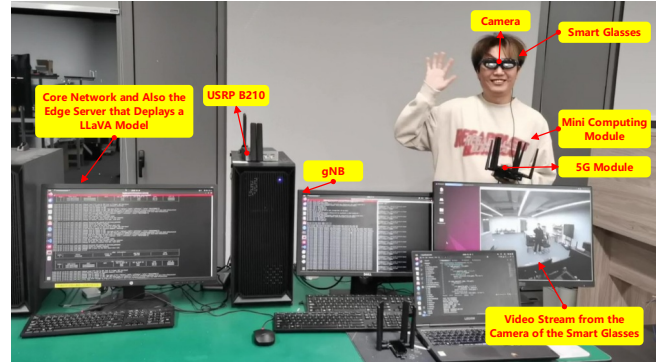


Figure 11. Smart glasses hardware integrates with the WiLLM wireless LLM service, following a typical UE-gNB-CN network architecture. The UE consists of customizable smart glasses and a Mini PC, which also houses the 5G module. A camera positioned at the glabella captures images, enabling collection and querying through a custom human-computer interaction logic.

study using augmented reality smart glasses as a resource-constrained terminal device requiring LLM integration. Figure. 11 illustrates the experimental setup, showing the hardware components of our custom smart glasses platform interfaced with WiLLM network infrastructure. The glasses feature a 5G module, computing unit, and camera capable of capturing visual data for LLM interpretation. This system enables users to query about scenes before them, allowing

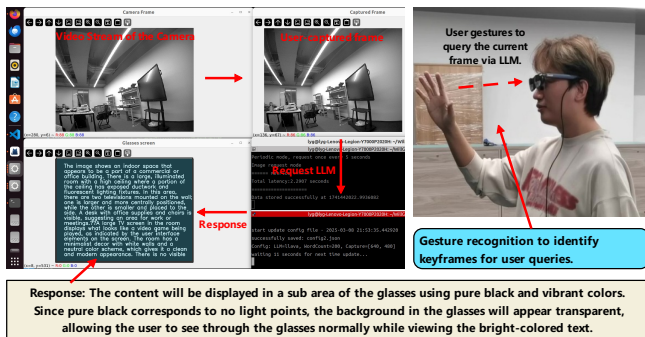


Figure 12. Gesture-triggered 5G LLM smart glasses data flow. The smart glasses application activates through embedded gesture recognition as the trigger. Upon detecting a five-finger extension followed by a grasping motion, the system captures the current visual feed and transmits it as a request to the LLM.

the LLM to interpret the visual context through a LLaVA model deployed in the core network host, accessed via gNB. **Key Validation:** The smart glasses implementation demonstrates a concrete manifestation of WiLLM’s “Tree-Branch-Fruit” slicing architecture, where the device functions primarily as a visual I/O interface while the computational workload is handled by GPU resources positioned at the network convergence point, as proposed in Section 3.

Figure. 12 shows the interactive paradigm between user and LLM service. The system uses gesture recognition to convert physical movements into contextual prompts for LLM processing, creating a bidirectional channel where gestures initiate queries and responses are displayed through the glasses’ interface.

6.2 Objective from an HCI Perspective

Human-computer interaction (HCI) research shows that interaction quality depends less on minimal latency than on consistent, predictable response patterns [17, 21]. Users adapt to predictable systems, but unpredictable delays disrupt interaction continuity. Our goal is to identify configurations that stabilize latency around 2 seconds for the smart glasses, balancing computational efficiency and perceptual continuity within wireless LLM constraints.

Empirical Insight: This case study revealed cross-layer dependencies where UE requests influenced communication resource utilization and allocation at the gNB, which affected LLM processing at the core network. This substantiates the complex relationships between resource allocation and performance documented in Section 5.

6.3 Approaches to Slice Optimization

We deployed two complementary methodologies to determine optimal slice configuration. Our offline approach utilized WiLLM’s data collection capabilities to analyze six slice configurations, identifying those that consistently maintained the 2-second latency target with minimal variance. Concurrently, we implemented an adaptive online learning framework using the UCB algorithm that continuously monitored performance metrics and dynamically adjusted

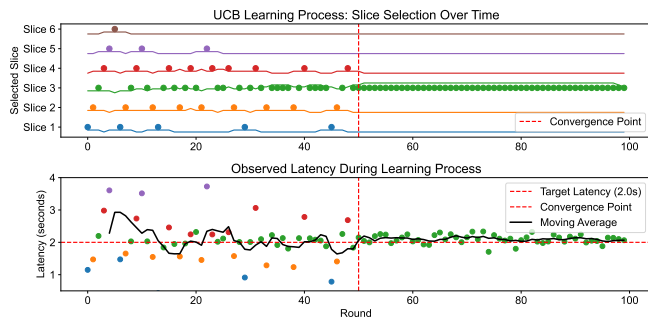


Figure 13. Online learning progress of the slice selection task for the smart glasses. Gradually converge to the target slice.

slice selection. As shown in Figure. 13, this method demonstrated progressive refinement toward optimal configuration with reduced latency fluctuations after convergence. While offline methods provided thorough validation requiring extensive initial data, online learning enabled adaptive optimization with initial exploration costs. Both approaches effectively identified suitable configurations, demonstrating WiLLM’s cross-layer optimization capabilities for resource-constrained applications.

Empirical Insight: The smart glasses case study provides empirical evidence that LLM service quality in wireless environments, particularly in some wearable HCI applications, depends more on maintaining predictable latency through intelligent slicing rather simply maximizing resources. While this single case offers only a directional indicator for resource-constrained applications, it demonstrates that WiLLM’s architectural principles effectively support interactive LLM experiences on computationally limited devices. Our dual optimization methodologies illustrate WiLLM’s availability of the dataset and cross-layer optimization potential, enabling sophisticated resource allocation tailored to specific application requirements. The hardware configurations and software components have been open-sourced to facilitate replication and expansion into other application areas.

7 Conclusion

WiLLM is the first open-source wireless system for LLM services. Our “Tree-Branch-Fruit” slicing architecture, LLMs deployment in CNs, and cross-layer APIs address limitations in existing wireless infrastructure for LLM delivery. The implementation extends OpenAirInterface with components enabling dynamic resource allocation, universal device compatibility, and multi-slice scheduling while preserving backward compatibility. A dataset of 1.6+ million synchronized metrics provides empirical foundation for research, while our smart glasses case demonstrates viability in resource-constrained environments. WiLLM connects telecom evolution with AI, enabling wireless LLM service chain optimization. Future research efforts will focus on addressing the current system’s deficiencies by prioritizing improvements in system stability and fault recovery, ensuring strict compliance with protocols, and implementing security measures for cross-layer APIs.

References

- [1] Maiko Andrade and Juliano Araujo Wickboldt. 2025. A Study on 5G Network Slice Isolation Based on Native Cloud and Edge Computing Tools. *arXiv preprint arXiv:2502.02842* (2025).
- [2] Maria Barbosa, Marcelo Silva, Ednelson Cavalcanti, and Kelvin Dias. 2024. Open-Source 5G Core Platforms: A Low-Cost Solution and Performance Evaluation. *arXiv preprint arXiv:2412.21162* (2024).
- [3] Lina Bariah, Qiyang Zhao, Hang Zou, Yu Tian, Faouzi Bader, and Merouane Debbah. 2024. Large generative ai models for telecom: The next big thing? *IEEE Communications Magazine* 62, 11 (2024), 84–90.
- [4] Gordon Owusu Boateng, Hani Sami, Ahmed Alagha, Hanae Elmekki, Ahmad Hammoud, Rabeb Mizouni, Azzam Mourad, Hadi Otrok, Jamal Bentahar, Sami Muhaidat, et al. 2024. A Survey on Large Language Models for Communication, Network, and Service Management: Application Insights, Challenges, and Future Directions. *arXiv preprint arXiv:2412.19823* (2024).
- [5] Fenglong Cai, Dong Yuan, Zhe Yang, and Lizhen Cui. 2024. Edge-llm: A collaborative framework for large language model serving in edge computing. In *2024 IEEE International Conference on Web Services (ICWS)*. IEEE, 799–809.
- [6] Abdelaali Chaoub and Muslim Elkotob. 2025. Mobile Network-specialized Large Language Models for 6G: Architectures, Innovations, Challenges, and Future Trends. *arXiv preprint arXiv:2502.04933* (2025).
- [7] Yuxuan Chen, Rongpeng Li, Xiaoxue Yu, Zhifeng Zhao, and Honggang Zhang. 2024. Adaptive layer splitting for wireless llm inference in edge computing: A model-based reinforcement learning approach. *arXiv preprint arXiv:2406.02616* (2024).
- [8] Yuxuan Chen, Rongpeng Li, Zhifeng Zhao, Chenghui Peng, Jianjun Wu, Ekram Hossain, and Honggang Zhang. 2024. NetGPT: An AI-native network architecture for provisioning beyond personalized generative services. *IEEE Network* (2024).
- [9] Abdulhalim Dandoush, Viswanath Kumarskandpriya, Mueen Uddin, and Usman Khalil. 2024. Large language models meet network slicing management and orchestration. *arXiv preprint arXiv:2403.13721* (2024).
- [10] Saeid K Dehkordi, Jan C Hauffen, Fabian Jaensch, Peter Jung, and Giuseppe Caire. 2023. Variational autoencoder-based parameter estimation in beam-space OFDM integrated sensing and communication. In *GLOBECOM 2023-2023 IEEE Global Communications Conference*. IEEE, 3904–3909.
- [11] Qifei Dong, Xiangliang Chen, and Mahadev Satyanarayanan. 2024. Creating edge ai from cloud-based llms. In *Proceedings of the 25th International Workshop on Mobile Computing Systems and Applications*. 8–13.
- [12] The Engineer. 2025. Expert Q&A: China’s new DeepSeek AI model. <https://www.theengineer.co.uk/content/in-depth/expert-q-and-a-chinas-new-deepseek-ai-model>.
- [13] Wojciech Flakowski, Maciej Krasicki, and Rafał Krenz. 2023. Implementation of a 4g/5g base station using the srsran software and the usrp software radio module. *Journal of Telecommunications and Information Technology* 3 (2023), 30–40.
- [14] Xenofon Foukas, Bozidar Radunovic, Matthew Balkwill, and Zhihua Lai. 2023. Taking 5G RAN analytics and control to a new level. In *Proceedings of the 29th Annual International Conference on Mobile Computing and Networking*. 1–16.
- [15] Ismael Gomez-Miguel, Andres Garcia-Saavedra, Paul D. Sutton, Pablo Serrano, Cristina Cano, and Douglas J. Leith. 2016. srsLTE: An Open-Source Platform for LTE Evolution and Experimentation. In *Proceedings of the Tenth ACM International Workshop on Wireless Network Testbeds, Experimental Evaluation, and Characterization (WiNTECH ’16)*. ACM, 25–32.
- [16] Ying He, Jingcheng Fang, F Richard Yu, and Victor C Leung. 2024. Large language models (LLMs) inference offloading and resource allocation in cloud-edge computing: An active inference approach. *IEEE Transactions on Mobile Computing* (2024).
- [17] Marco C Jacobs, Mark A Livingston, and Andrei State. 1997. Managing latency in complex augmented reality systems. In *Proceedings of the 1997 symposium on Interactive 3D graphics*. 49–ff.
- [18] Shashank Mohan Jain. 2022. Hugging face. In *Introduction to transformers for NLP: With the hugging face library and models to solve problems*. Springer, 51–67.
- [19] Boyi Liu, Jingwen Tong, and Jun Zhang. 2024. Llm-slice: Dedicated wireless network slicing for large language models. In *Proceedings of the 22nd ACM Conference on Embedded Networked Sensor Systems*. 853–854.
- [20] Purbesh Mitra, Priyanka Kaswan, and Sennur Ulukus. 2024. Distributed Mixture-of-Agents for Edge Inference with Large Language Models. *arXiv preprint arXiv:2412.21200* (2024).
- [21] Mahdi Nabiyouni, Siroberto Scerbo, Doug A Bowman, and Tobias Höllerer. 2017. Relative effects of real-world and virtual-world latency on an augmented reality training task: an ar simulation experiment. *Frontiers in ICT* 3 (2017), 34.
- [22] Sean Huver Nigel Nelson and Mostafa Toloui. 2023. Deploy Large Language Models at the Edge with NVIDIA IGX Orin Developer Kit.
- [23] Navid Nikaein, Mahesh K. Marina, Saravana Manickam, Alex Dawson, Raymond Knopp, and Christian Bonnet. 2014. OpenAirInterface: A Flexible Platform for 5G Research. *ACM SIGCOMM Computer Communication Review* 44, 5 (October 2014), 33–38.
- [24] NVIDIA. 2025. TensorRT-LLM: High-Performance Inference for Large Language Models. <https://github.com/NVIDIA/TensorRT-LLM>. Accessed: 2025-02-28.
- [25] Ollama. 2025. Ollama: An Open Source Project on GitHub. <https://github.com/ollama/ollama>. Accessed: 2025-02-28.
- [26] Open5GS. 2025. Open5GS: Open Source 5G Core Network. <https://open5gs.org/>. Accessed: 2025-02-28.
- [27] Jeff Rasley, Samyam Rajbhandari, Olatunji Ruwase, and Yuxiong He. 2020. DeepSpeed: System optimizations enable training deep learning models with over 100 billion parameters. In *Proceedings of the 26th ACM SIGKDD international conference on knowledge discovery & data mining*. 3505–3506.
- [28] Tony Saboorian and Amanda Xiang. 2017. Network Slicing and 3GPP Service and Systems Aspects (SA) Standard. *IEEE Software Defined Networks* (December 2017).
- [29] Robert Schmidt, Mikel Irazabal, and Navid Nikaein. 2021. FlexRIC: An SDK for next-generation SD-RANs. In *Proceedings of the 17th International Conference on emerging Networking EXperiments and Technologies*. 411–425.
- [30] Haotian Tang, Shang Yang, Ji Lin, Jiaming Tang, Wei-Ming Chen, Wei-Chen Wang, and Song Han. 2023. TinyChat: Large Language Model on the Edge. *MIT HAN Lab Blog* (2023). <https://hanlab.mit.edu/blog/tinychat>
- [31] Huaming Wu, Xiangyi Li, and Yingjun Deng. 2020. Deep learning-driven wireless communication for edge-cloud computing: opportunities and challenges. *Journal of Cloud Computing* 9, 1 (2020), 21.
- [32] Minrui Xu, Dusit Niyato, and Christopher G Brinton. 2025. Serving Long-Context LLMs at the Mobile Edge: Test-Time Reinforcement Learning-based Model Caching and Inference Offloading. *arXiv preprint arXiv:2501.14205* (2025).
- [33] Nan Xue, Yaping Sun, Zhiyong Chen, Meixia Tao, Xiaodong Xu, Liang Qian, Shuguang Cui, Wenjun Zhang, and Ping Zhang. 2024. WDMoE: Wireless Distributed Mixture of Experts for Large Language Models. *arXiv preprint arXiv:2411.06681* (2024).
- [34] Fangzhao You et al. 2024. JPPo: Joint Power and Prompt Optimization for Accelerated Large Language Model Services. *arXiv preprint* (2024).
- [35] Xiaoyu Zhang et al. 2025. Beyond the Cloud: Edge Inference for Generative Large Language Models in Wireless Networks. *IEEE Transactions on Wireless Communications* (2025).
- [36] Yue Zheng, Yuhao Chen, Bin Qian, Xiufang Shi, Yuanchao Shu, and Jiming Chen. 2024. A Review on edge large language models: Design, Execution, and Applications. *Comput. Surveys* (2024).

Appendix

A Appendix Overview

This appendix provides supplementary information, analysis, and technical details to support the main body of the paper. The contents are organized as follows: Appendix B presents a general comparison of WiLLM against existing open-source wireless communication systems and LLM deployment frameworks. This comparative analysis establishes WiLLM’s distinctive contributions within the telecommunications-AI convergence landscape.

Appendix C extends the comparative analysis through a granular examination of specific technical capabilities across contemporary wireless systems. This detailed evaluation substantiates WiLLM’s position as the first comprehensive system specifically designed for wireless LLM service delivery.

Appendix D illustrates the physical implementation of the WiLLM testbed, depicting the comprehensive hardware architecture that enables end-to-end LLM service delivery over wireless networks. It also showcases the WiLLM monitoring and performance analysis GUI, which provides real-time visualization and analytical capabilities for system optimization.

Appendix E details WiLLM’s hierarchical API architecture and presents the Tree-Branch-Fruit Slicing algorithm for UE resource allocation. These technical specifications elucidate the system’s cross-layer integration mechanisms and resource distribution methodologies.

Appendix F contains supplementary data analysis and visualizations from the WiLLM dataset. These figures provide deeper insights into the stability of experimental conditions, comparative performance between slice-enabled and normal traffic, and the complex interactions between various system parameters. More importantly, we conducted a causal analysis of the results shown in Figure 6 to Figure 10 of the dataset.

Appendix G introduces two novel benchmarking metrics - the LLM-Aware Resource Efficiency Index (LAREI) and the LLM Slice Efficiency Quotient (LSEQ). These metrics are derived from rigorous analysis of the WiLLM dataset and provide a comprehensive framework for evaluating the performance of LLM wireless communication systems.

Appendix H presents a comprehensive tabulation of all metrics collected in the WiLLM dataset across the UE, RAN, and Edge Server layers. This exhaustive catalog enables researchers to understand the full scope and granularity of the empirical data foundation provided by WiLLM.

The appendix aims to provide a rigorous technical foundation for the innovative architectural designs and empirical findings presented in the main paper. By offering detailed comparative analysis, comprehensive system specifications, in-depth dataset insights, and novel performance evaluation frameworks, this supplementary material enables researchers to fully engage with the technical contributions of WiLLM and build upon its open-source foundation to advance the state of the art in wireless LLM service delivery.

B Appendix for Section 2 (Related Work and Comparison): General Comparison of Systems

Table 1. Comparison of Open Source Wireless Communication Systems and LLM deployment Systems

System Name	Network Architecture	Slice Support	LLM Integration	Resource Scheduling	UE Compatibility	API Framework	Deployment Flexibility	Dataset & Benchmark
WiLLM	UE-gNB-CN with Edge Server	“Tree-Branch-Fruit” Slice	Designed specifically for LLM services	Dual-mode resource schedule	All UE	Cross-layer API framework	Core and edge part flexibility	✓
OAI [23]	UE-gNB-CN	Base slice	✗	Basic resource schedule	Slice-enabled UE	gNB Only	Traditional service-oriented	✗
srsRAN [13]	UE-gNB-CN	Base slice	✗	Flexible resource schedule	Slice-enabled UE	gNB Only	Traditional service-oriented	✗
Open5GS [26]	UE-gNB-CN	Base slice	✗	Basic resource schedule	Slice-enabled UE	gNB Only	Traditional service-oriented	✗
Hugging Face’s TGI [18]	LLM only	✗	Fine-tuning and optimization	✗	✗	Computation Only	Server	✗
Ollama [25]	LLM only	✗	LLM deployment	✗	✗	Computation Only	Server	✗
TensorRT-LLM [24]	LLM only	✗	Lightweight reasoning	✗	✗	Computation Only	Server	✗
DeepSpeed [27]	LLM only	✗	Distributed training and reasoning	✗	✗	Computation Only	Server	✗

Legend: ✓ Support ✗ Not Considered **Blue text:** key comparisons

Note: This comparison contrasts systems with different foundations: OAI, srsRAN, and Open5GS are ground-up implementations, while WiLLM strategically extends OAI’s architecture. While this may appear uneven, the comparison serves to highlight functional gaps in existing systems and how WiLLM addresses these through targeted extensions. This approach enables rapid innovation while leveraging established frameworks, demonstrating how focused architectural evolution can efficiently address emerging application needs.

Table 1 presents a comprehensive comparative analysis of WiLLM against existing open-source wireless communication systems and LLM deployment frameworks. This systematic evaluation establishes WiLLM’s distinctive contributions within the telecommunications-AI convergence landscape. While traditional systems (OAI, srsRAN, Open5GS) provide foundational wireless infrastructure components, they exhibit significant limitations in LLM integration capabilities. Concurrently, established LLM frameworks (Hugging Face’s TGI, Ollama, TensorRT-LLM, DeepSpeed) offer sophisticated model deployment but lack wireless communication integration. WiLLM uniquely bridges this interdisciplinary gap through its “Tree-Branch-Fruit” slicing architecture, cross-layer API framework, and universal UE compatibility mechanisms. This comparative evaluation demonstrates how WiLLM transcends the limitations of existing systems through its specialized design for LLM service delivery in wireless environments.

C Appendix for Section 2 (Related Work and Comparison): Detailed Technical Comparison of Systems

Table 2. Technical Comparison of Wireless Systems

Technical Features	WiLLM	OAI	srsRAN	Open5GS	FlexRIC	Janus
Type	LLM-Oriented Platform	Open-Source 5G System	Open-Source 4G/5G Suite	Open-Source 5G CN	Programmable RAN SDK	Programmable RAN Platform
Main Features	Specialized for LLM Comm.	Research and Prototyping	eNodeB and UE Apps	LTE/NR Core Network	xAPP Development	O-RAN Service Model
LLM-Specific Slicing Architecture	■	■	■	■	■	■
Dynamic Slice Compatibility	■	■	■	■	■	■
Universal UE Compatibility for Slice	■	■	■	■	■	■
Multi-UE-Multi-Slice Coordination	■	■	■	■	■	■
Dual-Mode Resource Scheduling	■	■	■	■	■	■
Cross-Layer API Framework	■	■	■	■	■	■
Flexible LLM Deployment	■	■	■	■	■	■
LLM Communication Dataset	■	■	■	■	■	■
LLM Communication Benchmark	■	■	■	■	■	■
Hierarchical Slice Policy Enforcement	■	■	■	■	■	■
Application-Layer Slice Access	■	■	■	■	■	■
Synchronized Multi-Interface Metrics	■	■	■	■	■	■
Offline and Online Slice Optimization	■	■	■	■	■	■
Programmability Interface	■	■	■	■	■	■
xApp/rApp Support	■	■	■	■	■	■
Disaggregated RAN Architecture	■	■	■	■	■	■
RAN Intelligence Controller Integration	■	■	■	■	■	■
Service Model Flexibility	■	■	■	■	■	■
Multi-vendor RAN Integration	■	■	■	■	■	■
Low-latency Optimization Tools	■	■	■	■	■	■
O-RAN Compliance	■	■	■	■	■	■
Protocol Strictness	■	■	■	■	■	■
Original Protocol Stack Implementation	■	■	■	■	■	■
Original Hardware Support	■	■	■	■	■	■
Original System Architecture	■	■	■	■	■	■
Open-Source Community Activity	■	■	■	■	■	■
Standard Compliance Testing Tools	■	■	■	■	■	■
Cost Efficiency for Deployment	■	■	■	■	■	■

Legend: ■ Full support/Good ■ Not supported/Bad ■ Partial support/Mediocre

Note: WiLLM is an extend of OAI

Table 2 extends our comparative analysis through a granular examination of specific technical capabilities across contemporary wireless systems. This evaluation reveals significant limitations in existing platforms regarding LLM service integration. While established systems like OAI, srsRAN, and Open5GS offer partial implementation of core wireless networking features, they demonstrate substantial deficiencies in specialized LLM communication capabilities. WiLLM distinguishes itself through full implementation of LLM-specific features, including dynamic slice compatibility, multi-UE-multi-slice coordination, and hierarchical slice policy enforcement. The matrix also highlights WiLLM’s innovative application-layer slice access mechanism, which enables universal device compatibility without requiring protocol-level modifications. This detailed technical comparison substantiates WiLLM’s position as the first comprehensive system specifically designed for wireless LLM service delivery.

D Appendix for Section 4 (System): The Hardware Platform

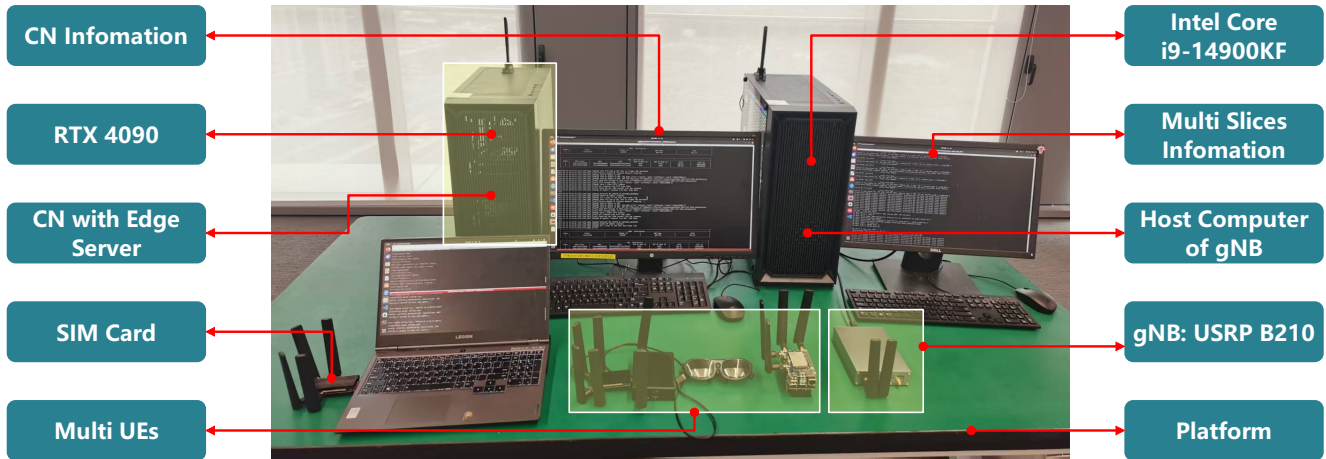


Figure 14. Hardware deployment of the WiLLM testbed, showcasing the integrated system with core network servers, edge computing nodes, Radio Access Network equipment, and multiple user terminal devices.

Figure 14 depicts the physical implementation of our WiLLM testbed, illustrating the comprehensive hardware architecture that enables end-to-end LLM service delivery over wireless networks. The deployment integrates multiple hierarchical components: an Intel Core i9-14900KF processor serving as the gNB host, a USRP B210 software-defined radio functioning as the RF frontend, and an NVIDIA RTX 4090 GPU enabling efficient LLM inference processing. The system supports simultaneous multi-slice and multi-UE operations through specialized hardware components and SIM card integration. This hardware configuration establishes a complete signal chain from core network to edge computing infrastructure, facilitating comprehensive experimental validation of the WiLLM architecture across diverse deployment scenarios and computational requirements.



Figure 15. WiLLM monitoring and performance analysis GUI, supporting multi-dimensional metric visualization, time-series analysis, and aggregate function computation.

Figure 15 illustrates the WiLLM monitoring and performance analysis GUI, which provides real-time visualization and analytical capabilities for system optimization. The interface implements a multi-dimensional metric visualization framework supporting time-series analysis and aggregate function computation. Key functional components include: (1) communication data display for real-time performance monitoring, (2) metrics selection interface for parameter filtering and comparison, (3) time interval selection for temporal analysis, (4) aggregate function selector for statistical computation, and (5) data selection mechanisms for customizing visualization parameters. This integrated monitoring framework enables comprehensive performance evaluation across multiple system layers, facilitating both runtime optimization and longitudinal performance analysis.

E Appendix for Section 4 (System): The API Architecture and Slice Algorithm of WiLLM

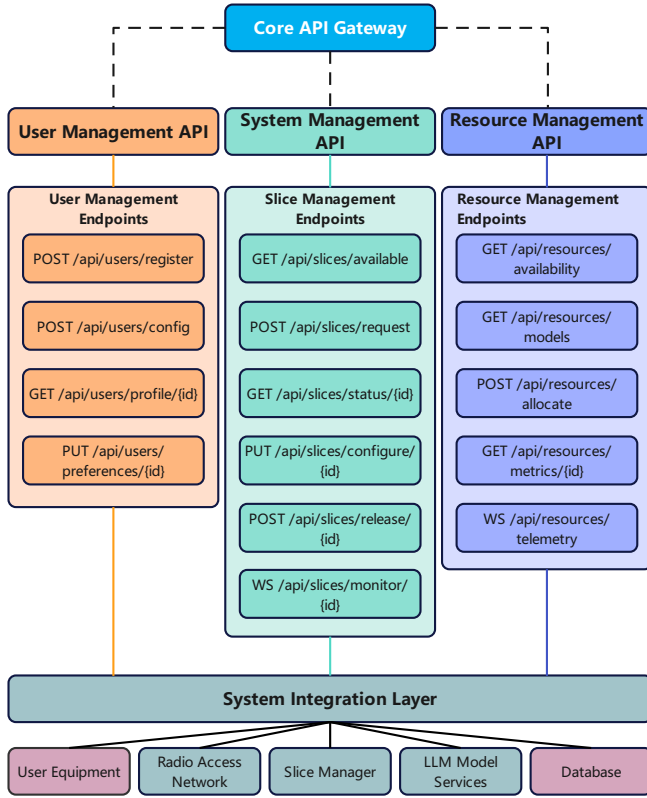


Figure 16. API Architecture of WiLLM.

Figure 16 illustrates WiLLM’s hierarchical API architecture with a three-tier structure: (1) User Management API handling registration, configuration and preferences; (2) System Management API orchestrating slice operations through availability checks, request processing, and status monitoring; and (3) Resource Management API managing resource discovery, allocation and telemetry. This architecture implements cross-layer integration while maintaining separation of concerns, using RESTful APIs for synchronous operations and WebSocket connections for asynchronous monitoring.

Algorithm 1 presents the Tree-Branch-Fruit Slicing algorithm for UE resource allocation. It processes UE identity, PRBs, slice policies, channel quality indicators, and throughput metrics through four phases: (1) branch slice determination using NSSAI configuration (lines 1-4); (2) transport block size computation with proportional fair metrics (lines 5-7); (3) hierarchical policy enforcement across branches and fruits (lines 8-13); and (4) final resource allocation with MCS selection (lines 14-16). This implementation ensures efficient resource distribution while maintaining slice isolation and service differentiation across multiple UEs.

Algorithm 1 Tree-Branch-Fruit Slicing for UEs

Require: UE u , total PRBs N_{PRB} , slice policies \mathcal{P} , channel quality parameters Q_m , R , n_{RB} , n_{sym} , L , and historical throughput $\Theta(u)$.

Ensure: Final allocated PRB count $R(u)$ and selected MCS for u .

1: /* **Determine UE’s branch slice based on NSSAI configuration** */

2: Define the slice set of u as

$$\mathcal{S}(u) = \{s \mid s \text{ is extracted from } \text{NSSAI}(u)\}$$

3: Compute the branch slice index

$$b = \text{MatchBranch}(\mathcal{S}(u), \mathcal{P})$$

4: Retrieve branch policy parameters:

$$\alpha_b^{\min} = \mathcal{P}(b). \text{min_ratio} \quad \& \quad \alpha_b^{\max} = \mathcal{P}(b). \text{max_ratio}$$

5: /* **Compute Transport Block Size using channel parameters** */

$$\text{TBS}(u) = f(Q_m, R, n_{\text{RB}}, n_{\text{sym}}, L)$$

6: Compute the proportional fair metric:

$$\gamma(u) = \frac{\text{TBS}(u)}{\Theta(u)}$$

7: Derive the initial allocation proportion via a function $\phi(\cdot)$:

$$r_{\text{init}} = N_{\text{PRB}} \cdot \phi(\gamma(u))$$

8: Enforce branch policy constraints (lower and upper):

$$r_{\text{branch}} = \min \left\{ r_{\text{init}}, N_{\text{PRB}} \cdot \alpha_b^{\max} \right\}$$

$$r_{\text{branch}} = \max \left\{ r_{\text{branch}}, N_{\text{PRB}} \cdot \alpha_b^{\min} \right\}$$

9: **if** a fruit mapping exists for u **then**

10: Let $(\pi(u), r_{\text{min}}, r_{\text{max}})$ be the fruit parameters for u .

11: **else**

12: Define default fruit parameters:

$$\pi(u) = 1, \quad r_{\text{min}} = N_{\text{PRB}} \cdot \alpha_b^{\min}, \quad r_{\text{max}} = N_{\text{PRB}} \cdot \alpha_b^{\max}$$

13: **end if**

14: Final resource allocation:

$$R(u) = \min \left\{ \max \left\{ \pi(u) \cdot r_{\text{branch}}, r_{\text{min}} \right\}, r_{\text{max}} \right\}$$

15: Determine MCS from channel conditions:

$$\text{MCS} = \text{SelectMCS}(u, Q_m, R, L)$$

16: **return** $(R(u), \text{MCS})$

F Appendix for Section 5 (Dataset)

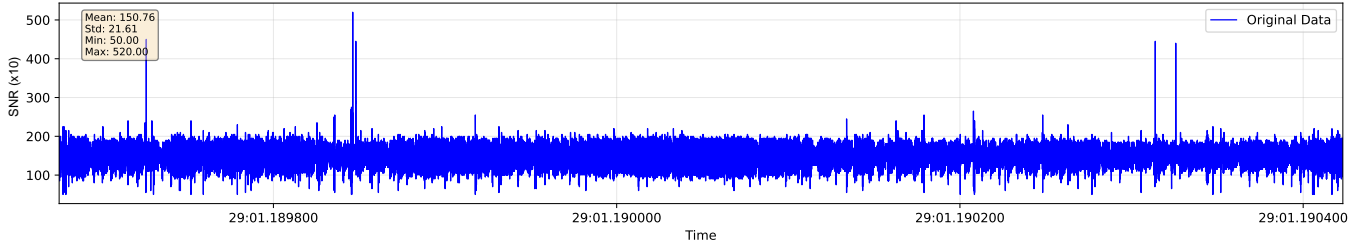


Figure 17. The variations in SNR during the data collection process.

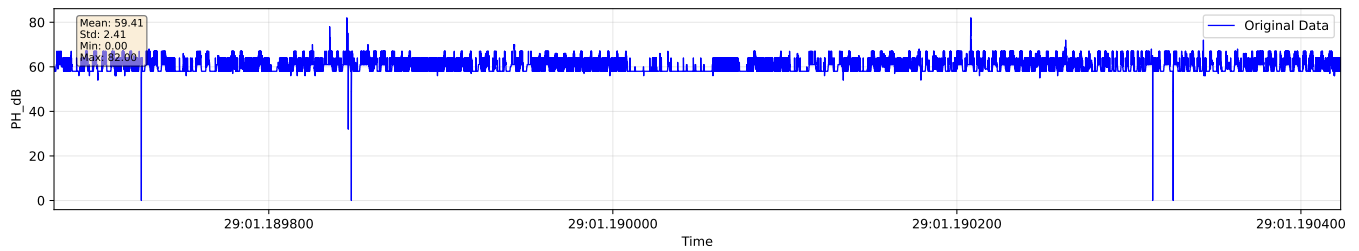


Figure 18. The variations in PH_dB during the data collection process.

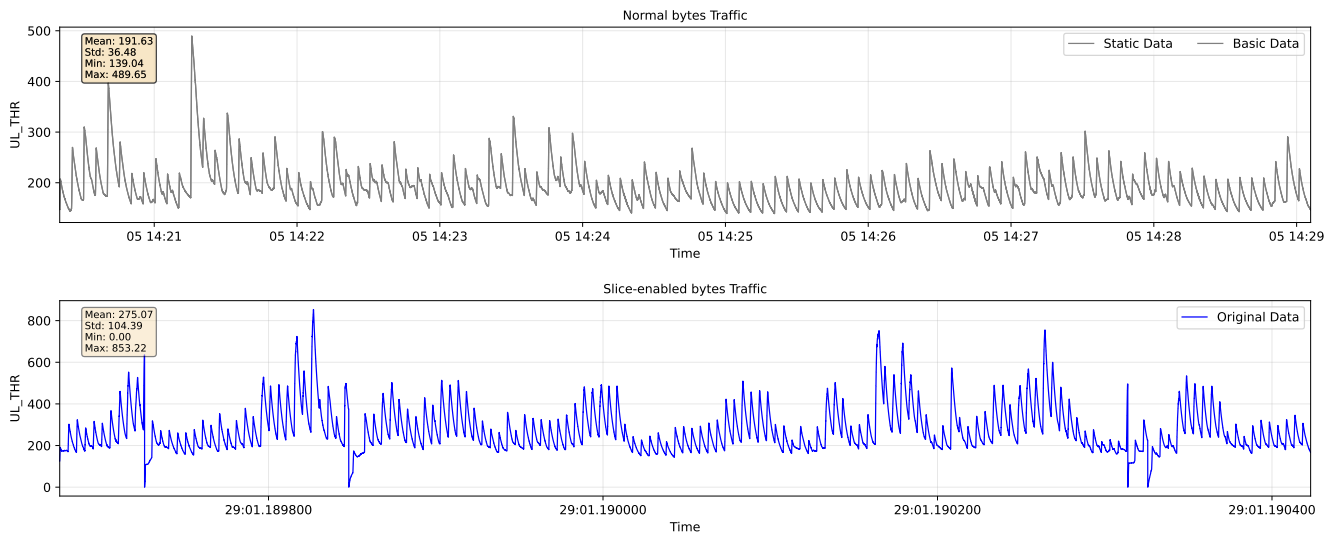


Figure 19. The variations in UL_THR during the data collection process.

Figures 17 and 18 present temporal analyses of Signal-to-Noise Ratio (SNR) and Power Headroom (PH_dB) variations during the data collection process, respectively. These visualizations demonstrate the stability of the experimental environment across multiple measurement dimensions. Figure 17 reveals consistent SNR levels (mean: 150.76, standard deviation: 21.61) across the data collection period, with minimal transient fluctuations, confirming reliable signal quality for experimental validity. Similarly, Figure 18 shows highly stable power headroom measurements (mean: 59.41, standard deviation: 2.41), indicating consistent UE transmission capabilities throughout the experimental process. These stability metrics validate the integrity of our dataset by confirming that the observed performance variations result from intentional experimental manipulations rather than environmental fluctuations or hardware inconsistencies.

Figure 19 displays comparative analyses of uplink throughput between normal traffic (top) and slice-enabled traffic (bottom) during the data collection process. The slice-enabled implementation demonstrates significantly higher average throughput compared to normal traffic, representing a 43.5% performance improvement. The slice-enabled approach also shows more

dynamic adaptation with higher peak throughput, enabling better responsiveness to varying service demands. While normal traffic exhibits regular but constrained patterns, the slice-enabled traffic shows more variable but overall superior performance characteristics with distinct periodic bursts that effectively utilize available bandwidth. This empirical evidence confirms that WiLLM’s slicing architecture successfully enhances throughput efficiency, allowing more responsive performance scaling for LLM services while maintaining an appropriate baseline throughput level, which is crucial for consistent user experience in latency-sensitive LLM applications.

F.1 Analysis of Uplink vs. Downlink Transmission Patterns (Figures 6, 7 and 8)

The differential performance profiles across slice configurations illustrated in Figure 8 substantiate the efficacy of WiLLM’s “Tree-Branch-Fruit” slicing architecture, with differences primarily attributable to input modality variations. The pronounced disparity in inference time contribution (11.6% to 59.6%) stems fundamentally from the computational asymmetry between processing graphical inputs in uplink scenarios versus textual inputs in downlink scenarios. Image-based queries in uplink transmissions necessitate substantially higher computational overhead for visual feature extraction, semantic interpretation, and multimodal reasoning, consequently dominating the latency profile. Conversely, text-based inputs in downlink scenarios require comparatively less computational intensity, shifting the performance bottleneck toward transmission components (28.9% to 54.7% variation in transmission time). This input-dependent computational variance underscores the necessity of WiLLM’s specialized slicing approach, which adaptively allocates resources based on modality-specific requirements rather than uniform distribution models. The statistically significant performance differentials between slices confirm that WiLLM effectively maintains service isolation while accommodating the inherent computational asymmetry between visual and textual processing pipelines, validating the fundamental premise of modality-optimized “Fruit Slices” within the hierarchical resource management framework.

It is important to note that our current implementation does not utilize specialized image generation models, which would likely introduce additional computational demands in the downlink scenario. Such models might shift the bottleneck toward inference processing rather than transmission, potentially altering the observed latency distribution patterns. Nevertheless, the empirical evidence clearly demonstrates that downlink image transmission presents a more significant bandwidth challenge than uplink image transmission, likely due to differences in compression efficiency and quality requirements between input and output images.

F.2 Resource Allocation-Utilization Relationship Analysis (Figures 9 and 10)

The non-linear correlation between PRB allocation patterns (Figure 9) and actual byte transmission volumes (Figure 10) reveals critical insights into resource utilization efficiency within wireless LLM service delivery. While WiLLM successfully implements differentiated PRB allocation conforming to slice policies, the observed discrepancy between allocated resources and realized throughput reflects complex cross-layer interdependencies spanning the entire system architecture. This phenomenon stems from multi-dimensional factors: (1) variable UE request patterns and buffer state fluctuations that create unpredictable traffic bursts; (2) server-side processing variability due to LLM inference time inconsistencies and computational resource contention; and (3) system execution mechanisms within the gNB layer, including scheduler implementation details, slice prioritization algorithms, and HARQ management policies. The visualization of slice-distinguished traffic with periodic transmission bursts demonstrates how these factors propagate across architectural boundaries, creating emergent system behaviors that cannot be predicted through isolated layer analysis. This empirical evidence substantiates the necessity of WiLLM’s cross-layer API framework, which enables coordinated adaptation across UE configuration, gNB resource allocation, and server processing prioritization based on observed end-to-end performance characteristics rather than theoretical layer-specific models—establishing a comprehensive feedback system essential for optimizing LLM service delivery in wireless environments.

F.3 Dataset Collection Parameters

F.3.1 UE Configuration Parameters

During data collection, we employed a configurable UE client with the following parameter ranges:

Our experiment controller dynamically adjusted these parameters with varying coefficients (1.0, 0.9, 0.8, 0.7, 0.6, 0.5) applied to the base resolutions to analyze performance across different capture qualities. This approach simulated diverse real-world usage scenarios with varying resource constraints and quality requirements.

F.3.2 Network Slicing Configuration

The network slicing configuration used in our experiments consisted of three primary slices with different resource allocation parameters. Three fruit slices were defined with max_ratio values of {30%, 60%, 90%}, all associated with the first parent slice. During data collection, our slice controller cycled through these configurations at 30-second intervals, updating the slice mapping for UEs to create varied resource allocation patterns throughout the dataset collection process.

Parameter	Description	Values
Image Capture Resolution	Resolution of images captured by smart glasses	320×240 to 640×480 pixels
Display Resolution	Resolution of the glasses display panel	800×600 to 1280×720 pixels
Request Mode	Type of request sent to LLM	“image_request”, “text_request”
LLM Model	Model used for inference	“llava”, “llama3.2”
Response Word Count	Maximum words requested in LLM response	50, 100, 150, 200 words
Request Frequency	Periodic request interval	5 seconds (default)

Table 3. UE configuration parameters used in dataset collection

G Benchmarking Metrics for LLM Wireless Communication

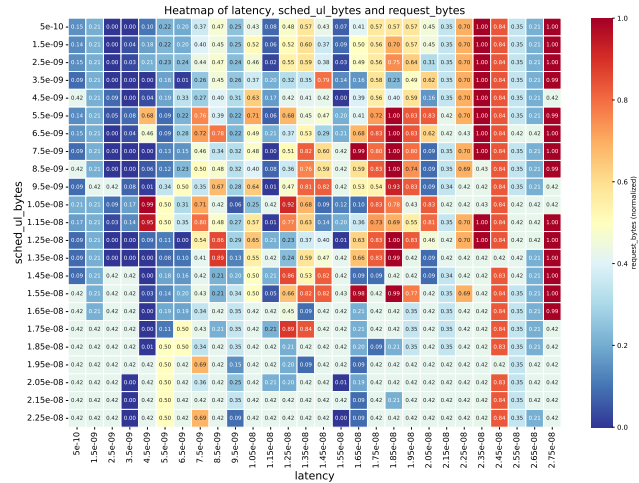


Figure 20. Latency, scheduled uplink bytes, and request bytes correlation heatmap. This figure presents a heatmap visualization of the complex interdependencies between latency, scheduled uplink bytes, and request bytes. The color-coded matrix reveals non-linear relationships between these parameters, identifying potential optimization opportunities and constraint boundaries that inform the development of comprehensive performance metrics for LLM wireless systems.

G.1 LLM-Aware Resource Efficiency Index

Based on Figure.20, our dataset analysis reveals complex interdependencies between latency, scheduled uplink bytes, and request bytes. The visualization demonstrates non-linear relationships between these critical parameters, suggesting the existence of multi-dimensional optimization boundaries that traditional isolated metrics fail to capture. The color-coded matrix illuminates several key observations:

- (1) Regions of optimal performance emerge at specific combinations of resource allocation and request volume, rather than following a monotonic improvement pattern with increasing resources.
- (2) Latency exhibits plateau effects at certain throughput thresholds, indicating saturation points where additional resources yield diminishing returns.
- (3) Request volume influences the relationship between resource allocation and latency in non-trivial ways, creating complex performance landscapes that require holistic optimization.

It is important to note that our heatmap representation, constrained by dimensionality limitations of visualization, necessarily focuses on three representative parameters. These selected metrics—latency, scheduled uplink bytes, and request bytes—serve as proxies for more complex system characteristics. For instance, scheduled uplink bytes approximate but do not completely capture overall resource utilization patterns across the network stack, while request bytes provide insight into workload demands without fully representing request resolution or complexity variations. Nevertheless, these parameters offer meaningful approximations of the fundamental system dynamics at play.

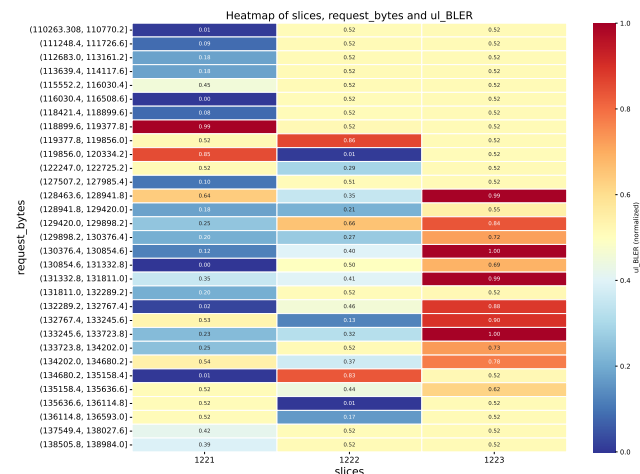


Figure 21. Correlation heatmap between slice configuration, request bytes, and uplink BLER. This figure presents a multi-dimensional analysis of how slice configuration, request payload size, and resulting error rates interact. The color-coded visualization provides empirical evidence for non-trivial relationships between these parameters, supporting the development of a slice efficiency index that balances resource allocation against transmission reliability.

To quantify these relationships, we propose the **LLM-Aware Resource Efficiency Index (LAREI)**, formulated as:

$$\text{LAREI} = \frac{\text{RDV} \cdot \log(1 + \text{LLM_Para})}{\text{Resources} \cdot \text{Latency}} \cdot \omega$$

Where:

- **RDV (Request Data Volume)** quantifies the amount of data requested by the user (approximated by request bytes in our dataset)
- **LLM_Para (LLM Parameter Count)** represents the computational complexity of the language model (measured in billions of parameters)
- **Resources (Allocated Communication Resources)** represents the network resources provisioned for transmission (approximated by scheduled uplink bytes)
- **Latency** measures end-to-end response time
- ω is a normalization coefficient that adjusts for system-specific characteristics

This formulation captures the fundamental efficiency relationship observed in our dataset while incorporating the computational dimension of LLM services. The logarithmic scaling of the parameter count acknowledges the empirically observed sub-linear relationship between model size and perceived quality improvements. This multidimensional index effectively balances the communication-computation trade-off inherent in LLM service delivery over wireless networks.

The LAREI serves as a comprehensive metric for evaluating resource allocation algorithms specifically tailored to LLM communication services, enabling researchers to identify optimal operating configurations that balance communication efficiency with model sophistication.

G.2 LLM Slice Efficiency Quotient

Figure. 9, Figure 10 and Figure. 21 reveal critical insights into network slicing performance that challenge conventional resource allocation assumptions. It demonstrates that higher resource allocation does not necessarily translate to proportionally lower error rates, suggesting an efficiency frontier in slice optimization. The comparative visualization of BLER between slice-enabled and normal traffic illustrates that excessive resource provisioning can potentially increase transmission errors.

Figure. 21 further illuminates this phenomenon through a correlation heatmap between slice configuration, request bytes, and uplink BLER. The visualization reveals distinct patterns where certain slice configurations exhibit superior error performance despite lower resource allocation, while others show degraded performance despite abundant resources. This empirical evidence supports the development of a slice efficiency metric that transcends simple resource allocation quantities.

It should be emphasized that our heatmap analysis, while instructive, represents a dimensional reduction of a multifaceted system. The three parameters visualized—slice configuration, request bytes, and BLER—function as indicative proxies for the broader system dynamics. For example, slice configuration encapsulates numerous implementation details not fully represented in the visualization, while BLER provides insight into transmission reliability without comprehensively capturing all aspects of service quality. Despite these limitations, the observed patterns reveal fundamental relationships that inform our metric development.

Based on these observations, we propose the **LLM Slice Efficiency Quotient (LSEQ)**:

$$\text{LSEQ} = \frac{\text{RDV_slice} \cdot (1 - \text{Error Rate}) \cdot \sqrt{\text{LLM_Para_slice}}}{\text{Slice Resources}} \cdot \delta$$

Where:

- **RDV_slice** represents the amount of data requested by users within the slice
- **Error Rate** quantifies transmission errors (represented by BLER in our dataset)
- **LLM_Para_slice** reflects the computational complexity of the language model deployed within the slice
- **Slice Resources** measures the communication resources provisioned to the slice
- δ is a calibration parameter that normalizes across different deployment scenarios

This formulation integrates the computational dimension of LLM services into the slice efficiency evaluation, recognizing that slices supporting more complex models (with higher parameter counts) deliver potentially higher service value. The square root scaling of parameter count reflects the diminishing returns observed in perceived quality as model size increases. The multiplicative error factor $(1 - \text{Error Rate})$ ensures that transmission reliability appropriately influences the efficiency evaluation, consistent with our empirical observations.

The LSEQ enables researchers to evaluate slicing algorithms specifically designed for LLM service delivery, accounting for the complex interplay between resource allocation, transmission reliability, and model sophistication. It provides a theoretically sound framework for optimizing slice configurations in LLM-oriented wireless communication systems.

H All Metrics of Dataset

Table 4. UE Layer Dataset Metrics

Layer	Metric	Description
UE	Timestamp	- Request initiation timestamp (Unix epoch milliseconds)
	Wireless Comm Time	- UE-gNB air interface duration (PDCP layer measurement)
	Total Comm Time	- UE-side end-to-end latency (request to response)
	Tx Image Resolution	- Original image dimensions (e.g., 1920×1080)
	Rx Image Resolution	- Received image dimensions post-processing
	Expected Word Count	- User-specified desired explanation length
	Actual Word Count	- LLM-generated response word count
	LLM Model	- Model architecture (LLaMA, LLaVA, etc.)
	Request Mode	- image_request or text_request
	Upload Periodicity	- Uplink interval (ms, 0=event-driven)
	Uplink Time	- UE-to-network latency (RLC layer)
	Downlink Time	- Network-to-UE latency (PDCP layer)
	Downlink Text Size	- Response payload size (UTF-8 bytes)
	Uplink Bytes	- Total bytes of the request (uplink)
Downlink Bytes	- Total bytes of the response (downlink)	

Table 5. Edge Server Layer Dataset Metrics

Layer	Metric	Description
Server	LLM Inference Time	- Model forward pass latency (ms)
	Server Processing Time	- Processing time in server
	Input Tokens	- Tokens consumed by LLM
	Output Tokens	- Tokens generated by LLM
	Cold Start Time	- Disk-to-RAM loading time
	Warm Start Time	- Cache reload time
	BLEU Score	- Text quality evaluation metric
	ROUGE Score	- Recall-based text evaluation
	Semantic Score	- Embedding similarity score
	GPU Utilization	- GPU compute usage (%)
	VRAM Usage	- Video memory consumption
	Downlink Image	- Base64 output image
	Response Text	- LLM-generated response

Table 6. RAN Layer Dataset Metrics

Layer	Metric	Description
RAN	gNB Timestamp	- gNB timestamp alignment (Unix epoch ms)
	Frame Number	- 5G NR system frame (0-1023)
	Slot Number	- Within-frame slot index (0-159)
	IMSI	- International Mobile Subscriber Identity
	RNTI	- Radio Network Temporary Identifier
	UE ID	- Device identifier within gNB
	UE Number	- Logical connection index
	DL Throughput	- Instantaneous downlink rate (Mbps)
	UL Throughput	- Instantaneous uplink rate (Mbps)
	PH (dB)	- UE Power Headroom report
	PCMAX (dBm)	- Max transmission power
	Avg RSRP	- Reference Signal Received Power
	CQI	- Channel Quality Indicator (0-15)
	RI	- MIMO Rank Indicator
	DL MCS	- Downlink Modulation and Coding Scheme
	UL MCS	- Uplink Modulation and Coding Scheme
	Scheduled UL Bytes	- Uplink buffer status
	Estimated UL Buffer	- gNB buffer estimation (bytes)
	DL PDUs Total	- Aggregated downlink PDUs
	DL BLER	- Downlink Block Error Rate (%)
	UL BLER	- Uplink Block Error Rate (%)
	DL-SCH Bytes	- Downlink shared channel payload
	DL-SCH RBs	- Downlink Resource Blocks allocated
	UL-SCH Bytes	- Uplink shared channel payload
	UL-SCH RBs	- Uplink Resource Blocks allocated
	UL MAC SDUs	- MAC Service Data Units count
	Primary Slice Max	- Main slice maximum resources
	Primary Slice Min	- Main slice minimum guarantee
	Secondary Slice Max	- Secondary slice maximum
	Secondary Slice Min	- Secondary slice minimum